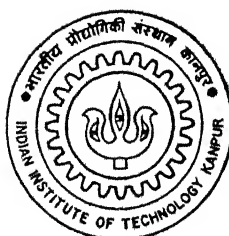


DESIGN & DEVELOPMENT OF C BAND MIXER USING DIELECTRIC RESONATORS

by

Major Pradeep Arora



DEPARTMENT OF ELECTRICAL ENGINEERING

INDIAN INSTITUTE OF TECHNOLOGY, KANPUR

MARCH, 1995

EE
1995
M
ARO
DES

DESIGN & DEVELOPMENT OF C BAND MIXER USING DIELECTRIC RESONATORS

A Thesis Submitted

in Partial Fulfillment of the Requirements

for the Degree of

Master of Technology

by

Major Pradeep Arora

to the

DEPARTMENT OF ELECTRICAL ENGINEERING
INDIAN INSTITUTE OF TECHNOLOGY, KANPUR

March 1995

24-000000/EE

1980年1月

EE-1995-M-ARO-DES

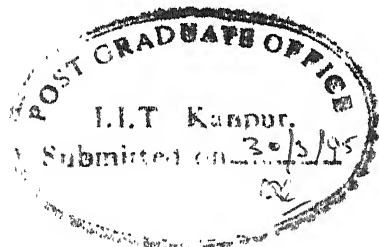


A121286

Certificate

It is certified that the work contained in the thesis entitled **DESIGN & DEVELOPMENT OF C BAND MIXER USING DIELECTRIC RESONATORS**, by Major Pradeep Arora, has been carried out under my supervision and that this work has not been submitted elsewhere for a degree.

30 March 1995



A handwritten signature in cursive script, likely belonging to Dr. Animesh Biswas.

Dr. Animesh Biswas

Asstt. Professor

Department of Electrical Engineering

I.I.T. Kanpur

Abstract

A C Band Microwave Mixer has been designed using dielectric resonators. The design is suited for MIC environment. The design makes use of dielectric resonators as series resonating elements for realizing signal and LO band pass filters. Modal analysis has been used to derive the field expressions for the suspended substrate structure. Information thus obtained has been used to calculate transmission characteristics of the microstrip line. Already available coupling information on microstrip line to dielectric resonator and dielectric resonator to dielectric resonator has been used in this design. A schottky barrier junction diode in self bias mode has been used as the mixer diode. The fabricated mixer is housed in a copper housing. A very sharp IF response has been obtained at the desired frequency using above design.

To
My Parents

Acknowledgements

I would take this opportunity to express my sincere gratitude towards Dr A Biswas, my thesis supervisor for having lit in my heart the flame symbolising the spirit of enquiry, for having encouraged me to make an attempt against all odds and for standing by me in my moments of sorrow and joy.

I thank my wife, my parents, my brother and my daughter for their staunch support.


I also thank Dr N C Mathur and Dr M Sachidananda for having laid threadbare the mystique and mysteries of Electromagnetics.

I also wish to express my sincere gratitude towards Dr B Bhat and Dr S K Koul, CARE IIT Delhi, for their having made available the necessary components for mixer fabrication.

I would cherish my association which I had forged here with Rajiv Shukla, Sridhar, Sriharsha, Harish, Apu and everybody else in the EM stream who were a great support during my thesis.

I would also remember the assistance extended by Mr Tiwari of departmental workshop, in fabrication of mixer housing.

Finally, I would be failing in my duty if I do not express my gratitude towards Corps of Signals who have afforded me this great opportunity.



Pradeep Arora

Contents

1	INTRODUCTION	1
1.1	Aim	1
1.2	Outline of Design Philosophy	1
1.3	Design Decisions	2
1.4	Organization of thesis	3
2	MODAL ANALYSIS	4
2.1	Introduction	4
2.2	Derivation of Electric and Magnetic Fields	4
2.3	Elements of Dyadic Green's Function Matrix	8
2.4	Determination of E_y , E_z , H_y , and H_z Field.	9
2.4.1	E_y in region 1, 2 and 3.	10
2.4.2	E_z in region 1, 2 and 3.	11
2.4.3	H_y in region 1, 2 and 3.	13
2.4.4	H_z in region 1, 2 and 3.	14
2.4.5	Summary of Field Expressions.	15
2.5	Application of the boundary conditions	18
2.5.1	Boundary conditions at $x = 0$	18
2.5.2	Boundary conditions at $x = -d$	19

2.6	Boundary Conditions at the plane of strip Conductor	25
2.7	Dispersion equations	29
3	MIXER DESIGN PRINCIPLES & PHILOSOPHY	34
3.1	Dielectric Resonators	34
3.1.1	Resonant frequency	36
3.1.2	Electromagnetic Field Coupling of a DR in MIC Configuration .	37
3.1.3	Coupling between two DRs	39
3.1.4	Frequency Tuning	41
3.2	Theory of a Band Pass Filter.	42
3.3	Theory of Mixers	44
3.3.1	Non linear solid state devices	48
3.3.2	Schottky barrier diode	48
3.3.3	GaAs MESFET	50
3.4	Types of Mixers	51
3.5	DR based Image recovery mixer	53
4	DR BASED MIXER REALIZATION	55
4.1	Outline design decisions	55
4.2	Transmission line parameters	56
4.3	Band pass filter design	57
4.3.1	RF BPF design	57
4.3.2	LO BPF Design	58
4.3.3	Impedence matching for the Diode	59
4.4	Mixer design	59
4.5	Tuning and performance improvement	60

5 CONCLUSION AND FUTURE DEVELOPMENTS

List of Figures

2.1	Suspended Substrate Structure	8
2.2	Qualified one term basis function satisfying edge condition at $ x = (\frac{w}{2})$	31
3.1	Field lines of the resonant mode $TE_{01\delta}$ in a DR	35
3.2	DR and microstrip line in MIC environment	38
3.3	DR coupled to microstrip transmission line	39
3.4	Modelling of DR - Mcrostrip line coupling.	40
3.5	Coupled DRs	41
3.6	Mode chart for Cylindrical DR.	42
3.7	External Quality Factor.	43
3.8	Coupling Coefficients.	44
3.9	Mechanical Tuning.	45
3.10	Equivalent circuit of a Band Pass Filter.	45
3.11	Schematic showing Schottky barrier Diode.	48
3.12	Equivalent Circuit of a Schottky Barrier Diode.	49
3.13	GaAs MESFET Schematic.	50
3.14	Various Types of Mixers.	51
3.15	FET Mixer.	52
3.16	Schematic of proposed Layout.	53

4.1	Layout of the Designed Mixer.	60
4.2	Noise Figure.	62
4.3	Conversion Loss.	63
4.4	$ S_{11} $ at RF Port.	64
4.5	Photograph showing the top view of the C Band Mixer.	65

List of Tables

3.1	Properties of Dielectric Resonators.	36
4.1	Transmission line Data.	57
4.2	Performance Data.	61

Chapter 1

INTRODUCTION

In [1] an image recovery mixer with a novel structure using dielectric resonators (DR's) for 22 GHz range has been proposed. Using this structure the image short condition for minimum noise figure has been easily obtained by the authors.

Concept behind the structure, can be usefully translated to work at other frequencies, depending on the application.

1.1 Aim

Aim of this thesis has been to realize a DR resonator based mixer in C Band. This could find an application in a C Band low noise down convertor for satellite broadcasting. Design principles, as calculated and collated in this thesis can act as suitable guidelines for fabrication at other frequencies.

1.2 Outline of Design Philosophy

A mixer essentially consists of two Band Pass filters and a nonlinear network. The Band Pass filters(BPF's) for both signal and Local oscillator frequencies utilize Dielectric resonators as series resonating elements. A Schottky Barrier mixer diode has been

used as a non-linear device to achieve mixing. A Broad Microstrip line has been used as IF filter.

The problem of design was broadly divided into following subparts and addressed as such

- a Accurate determination of transmission line parameters at the requisite frequencies,
- b Coupling parameters between the transmission line structure and the DR's, and between two DR's.
- c Band Pass filter design.
- d Mixer design and fabrication.
- e Performance improvement.

1.3 Design Decisions

Microstrip line was chosen as the transmission line because of ease of fabrication and easily obtainable coupling with dielectric resonators. A more generalized structure of suspended substrate was chosen for analysis and design. It afforded a distinct advantage in terms of tuning and fabrication.

Theoretically sound technique of Modal analysis has been used to derive propagation characteristics of the chosen structure. The microstrip line is magnetically coupled to DR's which have been excited in $TE_{01\delta}$ mode. Tight coupling between microstrip lines and DR's has been achieved by placing the resonators at odd number multiples of

a quarter of a guided wavelength at their resonant frequency from the open end of microstrip lines.

The Mixer was fabricated using a substrate of $\epsilon_r = 2.2$. It was enclosed in a copper housing. Other details about the mixer viz. Layout, its performance etc. have been elucidated in succeeding pages.

1.4 Organization of thesis

This thesis is organized as under:

After a brief introduction in chapter one, detailed modal analysis has been presented in chapter two. In third chapter mixer design principles and filter design have been dwelled upon. In fourth chapter design and development of DR based mixer, and results achieved find a mention. The thesis is concluded in fifth chapter with further suggestions.

Chapter 2

MODAL ANALYSIS

2.1 Introduction

In succeeding paras an attempt has been made to completely derive the Electric and Magnetic field expressions for the suspended substrate structure. Theoritcally sound technique of Modal analysis has been used to arrive at the requisite expressions.

2.2 Derivation of Electric and Magnetic Fields

Consider the electromagnetic field propagating in the +z direction and having x,z and time dependencies as $e^{-jk_x x}$, $e^{-j\beta z}$, and $e^{j\omega t}$ respectively. In a region containing no sources, this field satisfies the following Maxwell's eqautions:

$$\nabla \times \vec{H} = j\omega\epsilon_0\epsilon_r\vec{E} \quad (2.1)$$

$$\nabla \times \vec{E} = -j\omega\mu_0\vec{H} \quad (2.2)$$

where ϵ_r is the relative dielectric const of the medium and ϵ_0 is the dielectric const for the free space.

From 2.1 we get

$$\nabla \times \vec{H} = j\omega\epsilon_0\epsilon_r [E_x\hat{x} + E_y\hat{y} + E_z\hat{z}] \quad (2.3)$$

$$j\omega\epsilon_0\epsilon_r E_x = \frac{\partial H_z}{\partial y} - \frac{\partial H_y}{\partial z} \quad (2.4)$$

$$j\omega\epsilon_0\epsilon_r E_y = \frac{\partial H_x}{\partial z} - \frac{\partial H_z}{\partial x} \quad (2.5)$$

$$j\omega\epsilon_0\epsilon_r E_z = \frac{\partial H_y}{\partial x} - \frac{\partial H_x}{\partial y} \quad (2.6)$$

From 2.2 we get

$$\nabla \times \vec{E} = -j\omega\mu_0 [H_x\hat{x} + H_y\hat{y} + H_z\hat{z}] \quad (2.7)$$

$$-j\omega\mu_0 H_x = \frac{\partial E_z}{\partial y} - \frac{\partial E_y}{\partial z} \quad (2.8)$$

$$-j\omega\mu_0 H_y = \frac{\partial E_x}{\partial z} - \frac{\partial E_z}{\partial x} \quad (2.9)$$

$$-j\omega\mu_0 H_z = \frac{\partial E_y}{\partial x} - \frac{\partial E_x}{\partial y} \quad (2.10)$$

Substituting 2.6 in 2.9 we get

$$\begin{aligned} -j\omega\mu_0 H_y &= \frac{\partial E_x}{\partial z} - \frac{\partial}{\partial x} \left[\frac{1}{j\omega\epsilon_0\epsilon_r} \left[\frac{\partial H_y}{\partial x} - \frac{\partial H_x}{\partial y} \right] \right] \\ \omega^2\mu_0\epsilon_0\epsilon_r H_y &= j\omega\epsilon_0\epsilon_r \frac{\partial E_x}{\partial z} - \frac{\partial^2 H_y}{\partial x^2} + \frac{\partial^2 H_x}{\partial x\partial y} \end{aligned}$$

$$\left[\omega^2 \mu_0 \epsilon_0 \epsilon_r - k_x^2 \right] H_y = j\omega \epsilon_0 \epsilon_r \frac{\partial E_x}{\partial z} + \frac{\partial^2 H_x}{\partial x \partial y} \quad (2.11)$$

as $k_0^2 = \omega^2 \mu_0 \epsilon_0$

$$H_y = \frac{1}{k_0^2 \epsilon_r - k_x^2} \left[j\omega \epsilon_0 \epsilon_r \frac{\partial E_x}{\partial z} + \frac{\partial^2 H_x}{\partial x \partial y} \right] \quad (2.12)$$

Substituting 2.5 in 2.10 we get

$$\begin{aligned} -j\omega \mu_0 H_z &= -\frac{\partial E_x}{\partial y} + \frac{\partial}{\partial x} \left[\frac{1}{j\omega \epsilon_0 \epsilon_r} \left[\frac{\partial H_x}{\partial z} - \frac{\partial H_z}{\partial x} \right] \right] \\ \omega^2 \mu_0 \epsilon_0 \epsilon_r H_z &= -j\omega \epsilon_0 \epsilon_r \frac{\partial E_x}{\partial y} - \frac{\partial^2 H_z}{\partial x^2} + \frac{\partial^2 H_x}{\partial x \partial z} \\ \left[k_0^2 \epsilon_r - k_x^2 \right] H_z &= -j\omega \epsilon_0 \epsilon_r \frac{\partial E_x}{\partial y} + \frac{\partial^2 H_x}{\partial x \partial z} \end{aligned} \quad (2.13)$$

$$H_z = \frac{1}{k_0^2 \epsilon_r - k_x^2} \left[\frac{\partial^2 H_x}{\partial x \partial z} - j\omega \epsilon_0 \epsilon_r \frac{\partial E_x}{\partial y} \right] \quad (2.14)$$

Substituting 2.10 in 2.5 we get

$$\begin{aligned} j\omega \epsilon_0 \epsilon_r E_y &= \frac{\partial H_x}{\partial z} + \frac{\partial}{\partial x} \left[\frac{1}{-j\omega \mu_0} \left[\frac{\partial E_y}{\partial x} - \frac{\partial E_x}{\partial y} \right] \right] \\ \omega^2 \mu_0 \epsilon_0 \epsilon_r E_y &= -j\omega \mu_0 \frac{\partial H_x}{\partial z} - \frac{\partial^2 E_y}{\partial x^2} + \frac{\partial^2 E_x}{\partial x \partial y} \\ \left[k_0^2 \epsilon_r - k_x^2 \right] E_y &= -j\omega \mu_0 \frac{\partial H_x}{\partial z} + \frac{\partial^2 E_x}{\partial x \partial y} \end{aligned} \quad (2.15)$$

$$E_y = \frac{1}{k_0^2 \epsilon_r - k_x^2} \left[\frac{\partial^2 E_x}{\partial x \partial y} - j\omega \mu_0 \frac{\partial H_x}{\partial z} \right] \quad (2.16)$$

Substituting 2.9 in 2.6 we get

$$\begin{aligned}
 j\omega\epsilon_0\epsilon_r E_z &= -\frac{\partial H_x}{\partial y} + \frac{\partial}{\partial x} \left[\frac{1}{-j\omega\mu_0} \left[\frac{\partial E_x}{\partial z} - \frac{\partial E_z}{\partial x} \right] \right] \\
 \omega^2\mu_0\epsilon_0\epsilon_r E_z &= j\omega\mu_0 \frac{\partial H_x}{\partial y} - \frac{\partial^2 E_z}{\partial x^2} + \frac{\partial^2 E_x}{\partial x \partial z} \\
 [k_0^2 \epsilon_r - k_x^2] E_z &= j\omega\mu_0 \frac{\partial H_x}{\partial y} + \frac{\partial^2 E_x}{\partial x \partial z}
 \end{aligned} \tag{2.17}$$

$$E_z = \frac{1}{k_0^2 \epsilon_r - k_x^2} \left[\frac{\partial^2 E_x}{\partial x \partial z} + j\omega\mu_0 \frac{\partial H_x}{\partial y} \right] \tag{2.18}$$

On combining 2.12 and 2.14 vectorially we get

$$\begin{aligned}
 \vec{H}_t &= [\hat{y}H_y + \hat{z}H_z] \\
 \vec{H}_t &= \frac{1}{k_0^2 \epsilon_r - k_x^2} \left[\frac{\partial}{\partial x} \nabla_t H_x - j\omega\epsilon_0\epsilon_r \hat{x} \times \nabla_t E_x \right]
 \end{aligned} \tag{2.19}$$

On combining 2.16 and 2.18 vectorially we get

$$\begin{aligned}
 \vec{E}_t &= [\hat{y}E_y + \hat{z}E_z] \\
 \vec{E}_t &= \frac{1}{k_0^2 \epsilon_r - k_x^2} \left[\frac{\partial}{\partial x} \nabla_t E_x + j\omega\mu_0 \hat{x} \times \nabla_t H_x \right]
 \end{aligned} \tag{2.20}$$

from 2.19 and 2.20 , we can write

$$\begin{bmatrix} \vec{E}_t \\ \vec{H}_t \end{bmatrix} = \frac{1}{k_0^2 \epsilon_r - k_x^2} \begin{bmatrix} \frac{\partial}{\partial x} & j\omega\mu_0 \hat{x} \times \\ -j\omega\epsilon_0\epsilon_r \hat{x} \times & \frac{\partial}{\partial x} \end{bmatrix} \times \begin{bmatrix} \nabla_t E_x \\ \nabla_t H_x \end{bmatrix} \tag{2.21}$$

2.3 Elements of Dyadic Green's Function Matrix

The x components of the electric and magnetic fields satisfy the Helmholtz equation

$$\left[\frac{\partial^2}{\partial x^2} + \frac{\partial^2}{\partial y^2} + (k_0^2 \epsilon_r - \beta^2) \right] \begin{bmatrix} E_x \\ H_x \end{bmatrix} = 0 \quad (2.22)$$

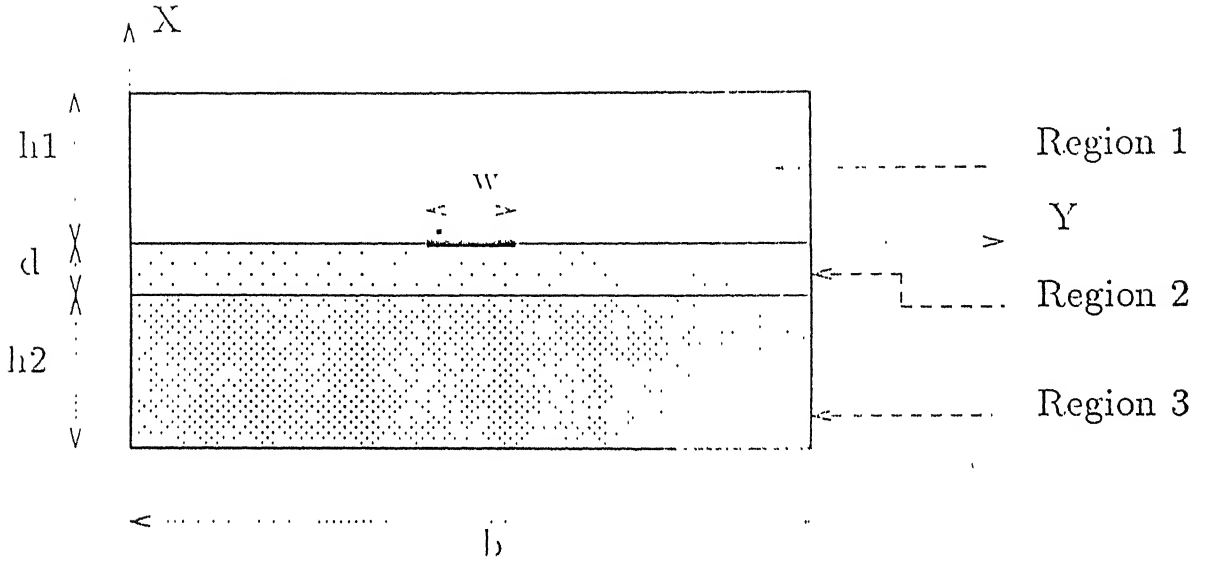


Figure 2.1: Suspended Substrate Structure

In Fig. 2.1 it is shown that entire structure can be divided into 3 regions. These have been referred to as region 1, 2 and 3 respectively. A very thin conductor lies on the boundary of region 1 and region 2. Thickness of the conductor is assumed to be much less than its width w . Thickness of each region is as shown in the Fig. . The structure is bounded by an Electric wall. For such a case solutions for E_x and H_x field distributions in each of the regions can be assumed as summation of all possible modes as under:

$$E_x^{(1)} = \sum_{n=1}^{\infty} A_{n1} \cos(\gamma_{n1}(x - h_1)) \sin(\alpha_{ny}) e^{-j\beta z} \quad (2.23)$$

$$E_x^{(2)} = \sum_{n=1}^{\infty} [A_{n2} \sin(\gamma_{n2} x) + A'_{n2} \cos(\gamma_{n2} x)] \sin(\alpha_n y) e^{-j\beta z} \quad (2.24)$$

$$E_x^{(3)} = \sum_{n=1}^{\infty} A_{n3} \cos(\gamma_{n3} (x + d + h_2)) \sin(\alpha_n y) e^{-j\beta z} \quad (2.25)$$

$$H_x^{(1)} = \sum_{n=0}^{\infty} B_{n1} \sin(\gamma_{n1} (x - h_1)) \cos(\alpha_n y) e^{-j\beta z} \quad (2.26)$$

$$H_x^{(2)} = \sum_{n=0}^{\infty} [B_{n2} \cos(\gamma_{n2} x) + B'_{n2} \sin(\gamma_{n2} x)] \cos(\alpha_n y) e^{-j\beta z} \quad (2.27)$$

$$H_x^{(3)} = \sum_{n=0}^{\infty} B_{n3} \sin(\gamma_{n3} (x + d + h_2)) \cos(\alpha_n y) e^{-j\beta z} \quad (2.28)$$

where the superscripts (1), (2) and (3) refer to region 1, 2 and 3 respectively and

$$\gamma_{n1} = \sqrt{k_0^2 - \alpha_n^2 - \beta^2}$$

$$\gamma_{n2} = \sqrt{k_0^2 \epsilon_{r2} - \alpha_n^2 - \beta^2}$$

$$\gamma_{n3} = \sqrt{k_0^2 \epsilon_{r3} - \alpha_n^2 - \beta^2}$$

$$\gamma_{n1} = k_{x1}$$

$$\gamma_{n1} = k_{x2}$$

$$\gamma_{n1} = k_{x3}$$

$$\epsilon_{r1} = 1$$

$$\alpha_n = k_{y1} = k_{y2} = k_{y3} = \frac{n\pi}{b}$$

2.4 Determination of E_y , E_z , H_y , and H_z Field.

Having assumed E_x and H_x field distributions as in equations 2.23 to 2.24 above expressions for E and H fields in y and z directions in each of the three regions can

be evaluated using the relations as derived in equations 2.12, 2.14, 2.16 and 2.18. The same have been evaluated in succeeding paras.

2.4.1 E_y in region 1, 2 and 3.

In region 1 the expression for E_y from eqn. 2.16 takes the form

$$E_y^{(1)} = \frac{1}{k_0^2 \epsilon_r - k_x^2} \left[\frac{\partial^2 E_x^{(1)}}{\partial x \partial y} - j\omega\mu_0 \frac{\partial H_x^{(1)}}{\partial z} \right] \quad (2.29)$$

From eqn. 2.23 and eqn. 2.26 on differentiating $E_x^{(1)}$ and $H_x^{(1)}$ we get

$$\frac{\partial^2 E_x^{(1)}}{\partial x \partial y} = [-\alpha_n A_{n1} \gamma_{n1} \sin(\gamma_{n1}(x - h_1)) \cos(\alpha_n y) e^{-j\beta z}] \quad (2.30)$$

$$\frac{\partial H_x^{(1)}}{\partial z} = -j\beta [B_{n1} \sin(\gamma_{n1}(x - h_1)) \cos(\alpha_n y) e^{-j\beta z}] \quad (2.31)$$

as for free space $\epsilon_r = 1$ we get $k_0^2 \epsilon_r - k_x^2 = \alpha_n^2 + \beta^2$ and eqn. 2.29 can now be written as under

$$E_y^{(1)} = \sum_{n=0}^{\infty} \frac{1}{\alpha_n^2 + \beta^2} [-\alpha_n A_{n1} \gamma_{n1} - \omega\beta\mu_0 B_{n1}] \sin(\gamma_{n1}(x - h_1)) \cos(\alpha_n y) e^{-j\beta z} \quad (2.32)$$

In region 2 the expression for E_y from eqn. 2.16 takes the form

$$E_y^{(2)} = \frac{1}{k_0^2 \epsilon_r - k_x^2} \left[\frac{\partial^2 E_x^{(2)}}{\partial x \partial y} - j\omega\mu_0 \frac{\partial H_x^{(2)}}{\partial z} \right] \quad (2.33)$$

From eqn. 2.24 and eqn. 2.27 on differentiating $E_x^{(2)}$ and $H_x^{(2)}$ we get

$$\frac{\partial^2 E_x^{(2)}}{\partial x \partial y} = [A_{n2} \alpha_n \gamma_{n2} \cos(\gamma_{n2} x) - A'_{n2} \alpha_n \gamma_{n2} \sin(\gamma_{n2} x)] \cos(\alpha_n y) e^{-j\beta z} \quad (2.34)$$

$$\frac{\partial H_x^{(2)}}{\partial z} = -j\beta[-j\omega\mu_0 B_{n_2} \cos(\gamma_{n_2} x) - j\omega\mu_0 B'_{n_2} \sin(\gamma_{n_2} x)] \cos(\alpha_n y) e^{-j\beta z} \quad (2.35)$$

$$\begin{aligned} E_y^{(2)} = & \sum_{n=0}^{\infty} \left[\frac{1}{\alpha_n^2 + \beta^2} [\alpha_n A_{n_2} \gamma_{n_2} - \omega\beta\mu_0 B_{n_2}] \cos(\gamma_{n_2} x) \right. \\ & \left. + \frac{1}{\alpha_n^2 + \beta^2} [-\alpha_n A'_{n_2} \gamma_{n_2} - \omega\beta\mu_0 B'_{n_2}] \sin(\gamma_{n_2} x) \right] \cos(\alpha_n y) e^{-j\beta z} \end{aligned} \quad (2.36)$$

In region 3 the expression for E_y from eqn. 2.16 takes the form

$$E_y^{(3)} = \frac{1}{k_0^2 \epsilon_r - k_x^2} \left[\frac{\partial^2 E_x^{(3)}}{\partial x \partial y} - j\omega\mu_0 \frac{\partial H_x^{(3)}}{\partial z} \right] \quad (2.37)$$

From eqn. 2.25 and eqn. 2.28 on differentiating $E_x^{(3)}$ and $H_x^{(3)}$ and combining the results we get

$$E_y^{(3)} = \sum_{n=0}^{\infty} \frac{1}{\alpha_n^2 + \beta^2} [-\alpha_n A_{n_3} \gamma_{n_3} - \omega\beta\mu_0 B_{n_3}] \sin(\gamma_{n_3} (x + d + h_2)) \cos(\alpha_n y) e^{-j\beta z} \quad (2.38)$$

2.4.2 E_z in region 1, 2 and 3.

In region 1 the expression for E_z from eqn. 2.18 takes the form

$$E_z^{(1)} = \frac{1}{k_0^2 \epsilon_r - k_x^2} \left[\frac{\partial^2 E_x^{(1)}}{\partial x \partial z} + j\omega\mu_0 \frac{\partial H_x^{(1)}}{\partial y} \right] \quad (2.39)$$

From eqn. 2.23 and eqn. 2.26 on differentiating $E_x^{(1)}$ and $H_x^{(1)}$ we get

$$\frac{\partial z E_x^{(1)}}{\partial x \partial z} = -j\beta A_{n_1} \gamma_{n_1} \sin(\gamma_{n_1} (x - h_1)) \sin(\alpha_n y) e^{-j\beta z} \quad (2.40)$$

$$\frac{\partial H_x^{(1)}}{\partial z} = -B_{n_1} \alpha_n \sin(\gamma_{n_1}(x - h_1)) \sin(\alpha_n y) e^{-j\beta z} \quad (2.41)$$

eqn. 2.23 can be written as under

$$E_z^{(1)} = \sum_{n=1}^{\infty} \frac{1}{\alpha_n^2 + \beta^2} [j\beta A_{n_1} \gamma_{n_1} - j\omega\mu_0 \alpha_n B_{n_1}] \sin(\gamma_{n_1}(x - h_1)) \sin(\alpha_n y) e^{-j\beta z} \quad (2.42)$$

In region 2 the expression for E_z from eqn. 2.18 takes the form

$$E_z^{(2)} = \frac{1}{k_0^2 \epsilon_r - k_x^2} \left[\frac{\partial^2 E_x^{(2)}}{\partial x \partial z} + j\omega\mu_0 \frac{\partial H_x^{(2)}}{\partial y} \right] \quad (2.43)$$

From eqn. 2.24 and eqn. 2.27 on differentiating and manipulating $E_x^{(2)}$ and $H_x^{(2)}$ we get

$$\begin{aligned} E_z^{(2)} = & \sum_{n=1}^{\infty} \left[\frac{1}{\alpha_n^2 + \beta^2} [-j\beta \gamma_{n_2} A_{n_2} - j\omega\mu_0 \alpha_n B_{n_2}] \cos(\gamma_{n_2} x) + \right. \\ & \left. \frac{1}{\alpha_n^2 + \beta^2} [j\beta \gamma_{n_2} A'_{n_2} - j\omega\mu_0 \alpha_n B'_{n_2}] \sin(\gamma_{n_2} x) \right] \sin(\alpha_n y) e^{-j\beta z} \end{aligned} \quad (2.44)$$

In region 3 the expression for E_z take the form

$$E_z^{(3)} = \frac{1}{k_0^2 \epsilon_r - k_x^2} \left[\frac{\partial^2 E_x^{(3)}}{\partial x \partial z} + j\omega\mu_0 \frac{\partial H_x^{(3)}}{\partial y} \right] \quad (2.45)$$

From eqn. 2.25 and eqn. 2.28 on differentiating $E_x^{(3)}$ and $H_x^{(3)}$ and combining the results we get

$$E_z^{(3)} = \sum_{n=1}^{\infty} \frac{1}{\alpha_n^2 + \beta^2} [j\beta \gamma_{n_3} A_{n_3} - j\omega\mu_0 \alpha_n B_{n_3}] \sin(\gamma_{n_3}(x + d + h_2)) \sin(\alpha_n y) e^{-j\beta z} \quad (2.46)$$

2.4.3 H_y in region 1, 2 and 3.

In region 1 the expression for H_y from eqn. 2.12 takes the form

$$H_y^{(1)} = \frac{1}{k_0^2 \epsilon_r - k_x^2} \left[j\omega \epsilon_0 \epsilon_{r1} \frac{\partial E_x^{(1)}}{\partial z} + \frac{\partial^2 H_x^{(1)}}{\partial x \partial y} \right] \quad (2.47)$$

From eqn. 2.23 and eqn. 2.26 on differentiating $E_x^{(1)}$ and $H_x^{(1)}$ we get

$$\frac{\partial^2 H_x^{(1)}}{\partial x \partial y} = \sum_{n=1}^{\infty} [-\alpha_n B_{n1} \gamma_{n1} \cos(\gamma_{n1}(x - h_1)) \sin(\alpha_n y) e^{-j\beta z}] \quad (2.48)$$

$$\frac{\partial E_x^{(1)}}{\partial z} = \sum_{n=0}^{\infty} [\beta \omega \epsilon_r \epsilon_0 A_{n1} \cos(\gamma_{n1}(x - h_1)) \sin(\alpha_n y) e^{-j\beta z}] \quad (2.49)$$

eqn. 2.47 now becomes

$$H_y^{(1)} = \sum_{n=1}^{\infty} \frac{1}{\alpha_n^2 + \beta^2} [-\alpha_n B_{n1} \gamma_{n1} + \omega \beta \epsilon_0 \epsilon_{r1} A_{n1}] \cos(\gamma_{n1}(x - h_1)) \sin(\alpha_n y) e^{-j\beta z} \quad (2.50)$$

In region 2 the expression for H_y takes the form

$$H_y^{(2)} = \frac{1}{k_0^2 \epsilon_r - k_x^2} \left[j\omega \epsilon_0 \epsilon_{r2} \frac{\partial E_x^{(2)}}{\partial z} + \frac{\partial^2 H_x^{(2)}}{\partial x \partial y} \right] \quad (2.51)$$

From eqn. 2.24 and eqn. 2.27 on differentiating $E_x^{(2)}$ and $H_x^{(2)}$ we get

$$\frac{\partial^2 H_x^{(2)}}{\partial x \partial y} = [B_{n2} \alpha_n \gamma_{n2} \sin(\gamma_{n2} x) - B'_{n2} \alpha_n \gamma_{n2} \cos(\gamma_{n2} x)] \sin(\alpha_n y) e^{-j\beta z} \quad (2.52)$$

$$\frac{\partial E_x^{(2)}}{\partial z} = -j\beta [A_{n2} \sin(\gamma_{n2} x) - A'_{n2} \cos(\gamma_{n2} x)] \sin(\alpha_n y) e^{-j\beta z} \quad (2.53)$$

$$H_y^{(2)} =$$

$$\begin{aligned} & \sum_{n=1}^{\infty} \left[\frac{1}{\alpha_n^2 + \beta^2} [\alpha_n \gamma_{n2} B_{n2} - \omega \beta \epsilon_0 \epsilon_{r2} A_{n2}] \sin(\gamma_{n2} x) \right. \\ & \left. + \frac{1}{\alpha_n^2 + \beta^2} [-\alpha_n \gamma_{n2} B'_{n2} + \omega \beta \epsilon_0 \epsilon_{r2} A'_{n2}] \cos(\gamma_{n2} x) \right] \sin(\alpha_n y) e^{-j\beta z} \end{aligned} \quad (2.54)$$

In region 3 the expression for H_y becomes

$$H_y^{(3)} = \frac{1}{k_0^2 \epsilon_r - k_x^2} \left[j\omega \epsilon_0 \epsilon_{r3} \frac{\partial E_x^{(3)}}{\partial z} + \frac{\partial^2 H_x^{(3)}}{\partial x \partial y} \right] \quad (2.55)$$

From eqn. 2.25 and eqn. 2.28 on differentiating $E_x^{(3)}$ and $H_x^{(3)}$ and combining the results we get

$$H_y^{(3)} = \sum_{n=1}^{\infty} \frac{1}{\alpha_n^2 + \beta^2} [-\alpha_n \gamma_{n3} B_{n3} + \omega \beta \epsilon_0 \epsilon_{r3} A_{n3}] \cos(\gamma_{n3} (x + d + h_2)) \sin(\alpha_n y) e^{-j\beta z} \quad (2.56)$$

2.4.4 H_z in region 1, 2 and 3.

In region 1 the expression for H_z from eqn. 2.14 takes the form

$$H_z^{(1)} = \frac{1}{k_0^2 \epsilon_r - k_x^2} \left[\frac{\partial^2 H_x^{(1)}}{\partial x \partial z} - j\omega \epsilon_0 \epsilon_{r1} \frac{\partial E_x^{(1)}}{\partial y} \right] \quad (2.57)$$

From eqn. 2.23 and eqn. 2.26 on differentiating $E_x^{(1)}$ and $H_x^{(1)}$ we get

$$\frac{\partial^2 H_x^{(1)}}{\partial x \partial z} = \sum_{n=0}^{\infty} -j\beta A_{n1} \gamma_{n1} \cos(\gamma_{n1} (x - h_1)) \cos(\alpha_n y) e^{-j\beta z} \quad (2.58)$$

$$\frac{\partial E_x^{(1)}}{\partial y} = \sum_{n=1}^{\infty} A_{n1} \alpha_n \cos(\gamma_{n1} (x - h_1)) \cos(\alpha_n y) e^{-j\beta z} \quad (2.59)$$

eqn. 2.57 can now be written as under

$$H_z^{(1)} = \sum_{n=1}^{\infty} \frac{1}{\alpha_n^2 + \beta^2} [-j\beta \gamma_{n1} B_{n1} - j\omega \epsilon_0 \epsilon_{r1} \alpha_n A_{n1}] \cos(\gamma_{n1} (x - h_1)) \cos(\alpha_n y) e^{-j\beta z} \quad (2.60)$$

In region 2 the expression for H_z from eqn. 2.18 takes the form

$$H_z^{(2)} = \frac{1}{k_0^2 \epsilon_r - k_x^2} \left[\frac{\partial^2 H_x^{(2)}}{\partial x \partial z} - j\omega \epsilon_0 \epsilon_{r2} \frac{\partial E_x^{(2)}}{\partial y} \right] \quad (2.61)$$

From eqn. 2.24 and eqn. 2.27 on differentiating and manipulating $E_x^{(2)}$ and $H_x^{(2)}$ we get

$$\begin{aligned} H_z^{(2)} = & \sum_{n=0}^{\infty} \left[\frac{1}{\alpha_n^2 + \beta^2} [j\beta \gamma_{n2} B_{n2} - j\omega \epsilon_0 \epsilon_{r2} \alpha_n A_{n2}] \sin(\gamma_{n2} x) \right. \\ & \left. + \frac{1}{\alpha_n^2 + \beta^2} [-j\beta \gamma_{n2} B'_{n2} - j\omega \epsilon_0 \epsilon_{r2} \alpha_n A'_{n2}] \cos(\gamma_{n2} x) \right] \cos(\alpha_n y) e^{-j\beta z} \end{aligned} \quad (2.62)$$

In region 3 the expression for H_z become

$$H_z^{(3)} = \frac{1}{k_0^2 \epsilon_r - k_x^2} \left[\frac{\partial^2 H_x^{(3)}}{\partial x \partial z} - j\omega \epsilon_0 \epsilon_{r3} \frac{\partial E_x^{(3)}}{\partial y} \right] \quad (2.63)$$

On differentiating $E_x^{(3)}$ and $H_x^{(3)}$ and combining the results we get

$$H_z^{(3)} = \sum_{n=1}^{\infty} \frac{1}{\alpha_n^2 + \beta^2} [-j\beta \gamma_{n3} B_{n3} - j\omega \epsilon_0 \epsilon_{r3} \alpha_n A_{n3}] \cos(\gamma_{n3} (x + d + h_2)) \cos(\alpha_n y) e^{-j\beta z} \quad (2.64)$$

2.4.5 Summary of Field Expressions.

Expressions for E_y , E_z , H_y , and H_z in each of the three regions derived in the previous subsection can be rewritten in following form:

Eqn. 2.32, 2.36, and 2.38 respectively become

$$E_y^{(1)} = \sum_{n=0}^{\infty} S_{n1} \sin(\gamma_{n1} (x - h_1)) \cos(\alpha_n y) e^{-j\beta z} \quad (2.65)$$

$$E_y^{(2)} = \sum_{n=0}^{\infty} [S_{n_2} \cos(\gamma_{n_2} x) + S'_{n_2} \sin(\gamma_{n_2} x)] \cos(\alpha_n y) e^{-j\beta z} \quad (2.66)$$

$$E_y^{(3)} = \sum_{n=0}^{\infty} S_{n_3} \sin(\gamma_{n_3} (x + d + h_2)) \cos(\alpha_n y) e^{-j\beta z} \quad (2.67)$$

where

$$\begin{aligned} S_{n_1} &= \frac{1}{\alpha_n^2 + \beta^2} [-\alpha_n A_{n_1} \gamma_{n_1} - \omega \beta \mu_0 B_{n_1}] \\ S_{n_2} &= \frac{1}{\alpha_n^2 + \beta^2} [\alpha_n A_{n_2} \gamma_{n_2} - \omega \beta \mu_0 B_{n_2}] \\ S'_{n_2} &= \frac{1}{\alpha_n^2 + \beta^2} [-\alpha_n A'_{n_2} \gamma_{n_2} - \omega \beta \mu_0 B'_{n_2}] \\ S_{n_3} &= \frac{1}{\alpha_n^2 + \beta^2} [-\alpha_n A_{n_3} \gamma_{n_3} - \omega \beta \mu_0 B_{n_3}] \end{aligned}$$

Eqn. 2.42, 2.44, and 2.46 respectively become

$$E_z^{(1)} = \sum_{n=1}^{\infty} C_{n_1} \sin(\gamma_{n_1} (x - h_1)) \sin(\alpha_n y) e^{-j\beta z} \quad (2.68)$$

$$E_z^{(2)} = \sum_{n=1}^{\infty} [C_{n_2} \cos(\gamma_{n_2} x) + C'_{n_2} \sin(\gamma_{n_2} x)] \sin(\alpha_n y) e^{-j\beta z} \quad (2.69)$$

$$E_z^{(3)} = \sum_{n=1}^{\infty} C_{n_3} \sin(\gamma_{n_3} (x + d + h_2)) \sin(\alpha_n y) e^{-j\beta z} \quad (2.70)$$

where

$$\begin{aligned} C_{n_1} &= \frac{1}{\alpha_n^2 + \beta^2} [j\beta A_{n_1} \gamma_{n_1} - j\omega \mu_0 \alpha_n B_{n_1}] \\ C_{n_2} &= \frac{1}{\alpha_n^2 + \beta^2} [-j\beta \gamma_{n_2} A_{n_2} - j\omega \mu_0 \alpha_n B_{n_2}] \\ C'_{n_2} &= \frac{1}{\alpha_n^2 + \beta^2} [j\beta \gamma_{n_2} A'_{n_2} - j\omega \mu_0 \alpha_n B'_{n_2}] \\ C_{n_3} &= \frac{1}{\alpha_n^2 + \beta^2} [j\beta \gamma_{n_3} A_{n_3} - j\omega \mu_0 \alpha_n B_{n_3}] \end{aligned}$$

Eqn. 2.50, 2.54, and 2.56 respectively become

$$H_y^{(1)} = \sum_{n=1}^{\infty} M_{n_1} \cos(\gamma_{n_1}(x - h_1)) \sin(\alpha_n y) e^{-j\beta z} \quad (2.71)$$

$$H_y^{(2)} = \sum_{n=1}^{\infty} [M_{n_2} \sin(\gamma_{n_2} x) + M'_{n_2} \cos(\gamma_{n_2} x)] \sin(\alpha_n y) e^{-j\beta z} \quad (2.72)$$

$$H_y^{(3)} = \sum_{n=1}^{\infty} M_{n_3} \cos(\gamma_{n_3}(x + d + h_2)) \sin(\alpha_n y) e^{-j\beta z} \quad (2.73)$$

where

$$\begin{aligned} M_{n_1} &= \frac{1}{\alpha_n^2 + \beta^2} [-\alpha_n B_{n_1} \gamma_{n_1} + \omega \beta \epsilon_0 A_{n_1}] \\ M_{n_2} &= \frac{1}{\alpha_n^2 + \beta^2} [\alpha_n \gamma_{n_2} B_{n_2} - \omega \beta \epsilon_0 \epsilon_{r_2} A_{n_2}] \\ M'_{n_2} &= \frac{1}{\alpha_n^2 + \beta^2} [-\alpha_n \gamma_{n_2} B'_{n_2} + \omega \beta \epsilon_0 \epsilon_{r_2} A'_{n_2}] \\ M_{n_3} &= \frac{1}{\alpha_n^2 + \beta^2} [-\alpha_n \gamma_{n_3} B_{n_3} + \omega \beta \epsilon_0 A_{n_3}] \end{aligned}$$

as $\epsilon_{r_1} = \epsilon_{r_3} = 1$ for region 1 and 3.

Eqn. 2.60, 2.62, and 2.64 respectively become

$$H_z^{(1)} = \sum_{n=1}^{\infty} D_{n_1} \cos(\gamma_{n_1}(x - h_1)) \cos(\alpha_n y) e^{-j\beta z} \quad (2.74)$$

$$H_z^{(2)} = \sum_{n=0}^{\infty} [D_{n_2} \sin(\gamma_{n_2} x) + D'_{n_2} \cos(\gamma_{n_2} x)] \cos(\alpha_n y) e^{-j\beta z} \quad (2.75)$$

$$H_z^{(3)} = \sum_{n=1}^{\infty} D_{n_3} \cos(\gamma_{n_3}(x + d + h_2)) \cos(\alpha_n y) e^{-j\beta z} \quad (2.76)$$

where

$$D_{n_1} = \frac{1}{\alpha_n^2 + \beta^2} [-j\beta \gamma_{n_1} B_{n_1} - j\omega \epsilon_0 \alpha_n A_{n_1}]$$

$$\begin{aligned}
D_{n_2} &= \frac{1}{\alpha_n^2 + \beta^2} [j\beta\gamma_{n_2} B_{n_2} - j\omega\epsilon_0\epsilon_{r_2}\alpha_n A_{n_2}] \\
D'_{n_2} &= \frac{1}{\alpha_n^2 + \beta^2} [-j\beta\gamma_{n_2} B'_{n_2} - j\omega\epsilon_0\epsilon_{r_2}\alpha_n A'_{n_2}] \\
D_{n_3} &= \frac{1}{\alpha_n^2 + \beta^2} [-j\beta\gamma_{n_3} B_{n_3} - j\omega\epsilon_0\alpha_n A_{n_3}]
\end{aligned}$$

2.5 Application of the boundary conditions

2.5.1 Boundary conditions at $x = 0$

Applying continuity conditions at $x = 0$

we have $H_x^{(1)} = H_x^{(2)}$ where

$$H_x^{(1)} = \sum_{n=0}^{\infty} B_{n_1} \sin(\gamma_{n_1}(x - h_1)) \cos(\alpha_n y) e^{-j\beta z}, \text{ and}$$

$$H_x^{(2)} = \sum_{n=0}^{\infty} [B_{n_2} \cos(\gamma_{n_2} x) + B'_{n_2} \sin(\gamma_{n_2} x)] \cos(\alpha_n y) e^{-j\beta z}$$

putting $x = 0$ in above expressions we get

$$\sum_{n=0}^{\infty} B_{n_1} \sin(-\gamma_{n_1} h_1) = \sum_{n=0}^{\infty} B_{n_2}$$

thus we obtain an expression for B_{n_2} in terms of B_{n_1} as under

$$B_{n_2} = -B_{n_1} \sin(\gamma_{n_1} h_1) \quad (2.77)$$

also at $x = 0$ we have $E_y^{(1)} = E_y^{(2)}$ i. e.

$$E_y^{(1)} = \sum_{n=0}^{\infty} S_{n_1} \sin(\gamma_{n_1}(x - h_1)) \cos(\alpha_n y) e^{-j\beta z}, \text{ and}$$

$$E_y^{(2)} = \sum_{n=0}^{\infty} [S_{n_2} \cos(\gamma_{n_2} x) + S'_{n_2} \sin(\gamma_{n_2} x)] \cos(\alpha_n y) e^{-j\beta z}$$

are continuous. On equating these expressions we get

$$S_{n_1} \sin(\gamma_{n_1} h_1) = S_{n_2}$$

after substituting the values of S_{n_1} and S_{n_2} this can be simplified as under

$$-\frac{1}{\alpha_n^2 + \beta^2} [-\alpha_n A_{n_1} \gamma_{n_1} - \omega\beta\mu_0 B_{n_1}] \sin(\gamma_{n_1} h_1) = \frac{1}{\alpha_n^2 + \beta^2} [\alpha_n A_{n_2} \gamma_{n_2} - \omega\beta\mu_0 B_{n_2}]$$

putting the value of B_{n_2} from eqn 2.77 and upon simplification of above expression

we get

$$A_{n_1} \alpha_n \gamma_{n_1} = \frac{\alpha_n A_{n_2} \gamma_{n_2}}{\sin(\gamma_{n_1} h_1)}$$

we finally obtain an expression for A_{n_2} in terms of A_{n_1} as under

$$A_{n_2} = A_{n_1} \frac{\gamma_{n_1}}{\gamma_{n_2}} \sin(\gamma_{n_1} h_1) \quad (2.78)$$

2.5.2 Boundary conditions at $x = -d$

Now Applying continuity equations at $x = -d$ we have

$$E_y^{(2)} = E_y^{(3)} \text{ and } E_z^{(2)} = E_z^{(3)}$$

Taking the E_y component first

$$E_y^{(2)} = \sum_{n=0}^{\infty} [S_{n_2} \cos(\gamma_{n_2} x) + S'_{n_2} \sin(\gamma_{n_2} x)] \cos(\alpha_n y) e^{-\beta z}$$

$$E_y^{(3)} = \sum_{n=0}^{\infty} S_{n_3} \sin(\gamma_{n_3} (x + d + h_2)) \cos(\alpha_n y) e^{-\beta z}$$

at $x = -d$ above expression when equated become

$$[S_{n_2} \cos(-\gamma_{n_2} d) + S'_{n_2} \sin(-\gamma_{n_2} d)] = S_{n_3} \sin(\gamma_{n_3} h_2)$$

$$\begin{aligned} \frac{1}{\alpha_n^2 + \beta^2} [\alpha_n A_{n_2} \gamma_{n_2} - \omega \beta \mu_0 B_{n_2}] \cos(\gamma_{n_2} d) - \frac{1}{\alpha_n^2 + \beta^2} [-\alpha_n A'_{n_2} \gamma_{n_2} - \omega \beta \mu_0 B'_{n_2}] \sin(\gamma_{n_2} d) = \\ \frac{1}{\alpha_n^2 + \beta^2} [-\alpha_n A_{n_3} \gamma_{n_3} - \omega \beta \mu_0 B_{n_3}] \sin(\gamma_{n_3} h_2) \end{aligned}$$

This can be rewritten as

$$\begin{aligned} \frac{1}{\alpha_n^2 + \beta^2} [-\alpha_n A_{n_3} \gamma_{n_3} - \omega \beta \mu_0 B_{n_3}] = \\ \frac{1}{\alpha_n^2 + \beta^2} [\alpha_n A_{n_2} \gamma_{n_2} - \omega \beta \mu_0 B_{n_2}] \frac{\cos(\gamma_{n_2} d)}{\sin(\gamma_{n_3} h_2)} \\ - \frac{1}{\alpha_n^2 + \beta^2} [-\alpha_n A'_{n_2} \gamma_{n_2} - \omega \beta \mu_0 B'_{n_2}] \frac{\sin(\gamma_{n_2} d)}{\sin(\gamma_{n_3} h_2)} \end{aligned} \quad (2.79)$$

Now equating the E_z component

$$E_z^{(2)} = \sum_{n=1}^{\infty} [C_{n_2} \cos(\gamma_{n_2} x) + C'_{n_2} \sin(\gamma_{n_2} x)] \sin(\alpha_n y) e^{-\beta z}, \text{ and}$$

$$E_z^{(3)} = \sum_{n=1}^{\infty} C_{n_3} \sin(\gamma_{n_3} (x + d + h_2)) \sin(\alpha_n y) e^{-\beta z}$$

at $x = -d$ we get

$$C_{n_2} \cos(\gamma_{n_2} d) - C'_{n_2} \sin(\gamma_{n_2} d) = C_{n_3} \sin(\gamma_{n_3} h_2)$$

$$\begin{aligned} & \frac{1}{\alpha_n^2 + \beta^2} [-j\beta\gamma_{n_2} A_{n_2} - j\omega\mu_0\alpha_n B_{n_2}] \cos(\gamma_{n_2} d) - \frac{1}{\alpha_n^2 + \beta^2} [j\beta\gamma_{n_2} A'_{n_2} - j\omega\mu_0\alpha_n B'_{n_2}] \sin(\gamma_{n_2} d) \\ &= \frac{1}{\alpha_n^2 + \beta^2} [j\beta\gamma_{n_3} A_{n_3} - j\omega\mu_0\alpha_n B_{n_3}] \sin(\gamma_{n_3} h_2) \end{aligned}$$

This can be rewritten as

$$\begin{aligned} & \frac{1}{\alpha_n^2 + \beta^2} [j\beta\gamma_{n_3} A_{n_3} - j\omega\mu_0\alpha_n B_{n_3}] = \\ & \frac{1}{\alpha_n^2 + \beta^2} [-j\beta\gamma_{n_2} A_{n_2} - j\omega\mu_0\alpha_n B_{n_2}] \frac{\cos(\gamma_{n_2} d)}{\sin(\gamma_{n_3} h_2)} \\ & - \frac{1}{\alpha_n^2 + \beta^2} [-j\beta\gamma_{n_2} A'_{n_2} - j\omega\mu_0\alpha_n B'_{n_2}] \frac{\sin(\gamma_{n_2} d)}{\sin(\gamma_{n_3} h_2)} \end{aligned} \quad (2.80)$$

$$\begin{aligned} & \begin{bmatrix} -\alpha_n\gamma_{n_3} & -\omega\beta\mu_0 \\ j\beta\gamma_{n_3} & -j\omega\mu_0\alpha_n \end{bmatrix} \begin{bmatrix} A_{n_3} \\ B_{n_3} \end{bmatrix} = \\ & \begin{bmatrix} \alpha_n\gamma_{n_2} & -\omega\beta\mu_0 & \alpha_n\gamma_{n_2} & \omega\beta\mu_0 \\ -j\beta\gamma_{n_2} & -j\omega\mu_0\alpha_n & -j\beta\gamma_{n_2} & j\omega\mu_0\alpha_n \end{bmatrix} \begin{bmatrix} A_{n_2} \frac{\cos(\gamma_{n_2} d)}{\sin(\gamma_{n_3} h_2)} \\ B_{n_2} \frac{\cos(\gamma_{n_2} d)}{\sin(\gamma_{n_3} h_2)} \\ A'_{n_2} \frac{\sin(\gamma_{n_2} d)}{\sin(\gamma_{n_3} h_2)} \\ B'_{n_2} \frac{\sin(\gamma_{n_2} d)}{\sin(\gamma_{n_3} h_2)} \end{bmatrix} \end{aligned} \quad (2.81)$$

Taking the coeff matrix of A_{n_3} and B_{n_3} to the right hand side of the expression, we get

$$\begin{aligned} & \begin{bmatrix} A_{n_3} \\ B_{n_3} \end{bmatrix} = \frac{1}{j\omega\mu_0\gamma_{n_3}(\alpha_n^2 + \beta^2)} \begin{bmatrix} -j\omega\mu_0\alpha_n & \omega\beta\mu_0 \\ -j\beta\gamma_{n_3} & \alpha_n\gamma_{n_3} \end{bmatrix} \times \\ & \begin{bmatrix} \alpha_n\gamma_{n_2} & -\omega\beta\mu_0 & \alpha_n\gamma_{n_2} & \omega\beta\mu_0 \\ -j\beta\gamma_{n_2} & -j\omega\mu_0\alpha_n & -j\beta\gamma_{n_2} & j\omega\mu_0\alpha_n \end{bmatrix} \begin{bmatrix} A_{n_2} \frac{\cos(\gamma_{n_2} d)}{\sin(\gamma_{n_3} h_2)} \\ B_{n_2} \frac{\cos(\gamma_{n_2} d)}{\sin(\gamma_{n_3} h_2)} \\ A'_{n_2} \frac{\sin(\gamma_{n_2} d)}{\sin(\gamma_{n_3} h_2)} \\ B'_{n_2} \frac{\sin(\gamma_{n_2} d)}{\sin(\gamma_{n_3} h_2)} \end{bmatrix} \end{aligned}$$

This can be written as

$$\begin{bmatrix} A_{n3} \\ B_{n3} \end{bmatrix} = \frac{1}{j\omega\mu_0\gamma_{n3}p} \times \begin{bmatrix} -j\omega\mu_0\gamma_{n2}p & 0 & -j\omega\mu_0\gamma_{n2}p & 0 \\ 0 & j\omega\mu_0\gamma_{n3}p & 0 & -j\omega\mu_0\gamma_{n3}p \end{bmatrix} \begin{bmatrix} A_{n2} \frac{\cos(\gamma_{n2}d)}{\sin(\gamma_{n3}h_2)} \\ B_{n2} \frac{\cos(\gamma_{n2}d)}{\sin(\gamma_{n3}h_2)} \\ A'_{n2} \frac{\sin(\gamma_{n2}d)}{\sin(\gamma_{n3}h_2)} \\ B'_{n2} \frac{\sin(\gamma_{n2}d)}{\sin(\gamma_{n3}h_2)} \end{bmatrix}$$

where $p = (\alpha_n^2 + \beta^2)$

$$\begin{bmatrix} A_{n3} \\ B_{n3} \end{bmatrix} = \begin{bmatrix} \frac{-\gamma_{n2}}{\gamma_{n3}} & 0 & \frac{-\gamma_{n2}}{\gamma_{n3}} & 0 \\ 0 & 1 & 0 & -1 \end{bmatrix} \times \begin{bmatrix} A_{n2} \frac{\cos(\gamma_{n2}d)}{\sin(\gamma_{n3}h_2)} \\ B_{n2} \frac{\cos(\gamma_{n2}d)}{\sin(\gamma_{n3}h_2)} \\ A'_{n2} \frac{\sin(\gamma_{n2}d)}{\sin(\gamma_{n3}h_2)} \\ B'_{n2} \frac{\sin(\gamma_{n2}d)}{\sin(\gamma_{n3}h_2)} \end{bmatrix} \quad (2.82)$$

Now considering the H Field at the boundary $x = -d$, we have

$$H_y^{(2)} = H_y^{(3)}, \text{ and}$$

$$H_z^{(2)} = H_z^{(3)}$$

Taking the $H_y^{(2)}$ and $H_y^{(3)}$ expressions, we have

$$H_y^{(2)} = \sum_{n=1}^{\infty} [M_{n2} \sin(\gamma_{n2}x) + M'_{n2} \cos(\gamma_{n2}x)] \sin(\alpha_n y) e^{-j\beta z}$$

$$H_y^{(3)} = \sum_{n=1}^{\infty} M_{n3} \cos(\gamma_{n3}(x + d + h_2)) \sin(\alpha_n y) e^{-j\beta z}$$

at $x = -d$ above expressions become

$$H_y^{(2)} = \sum_{n=1}^{\infty} [M_{n2} \sin(-\gamma_{n2}d) + M'_{n2} \cos(-\gamma_{n2}d)] \sin(\alpha_n y) e^{-j\beta z}$$

$$H_y^{(3)} = \sum_{n=1}^{\infty} [M_{n3} \cos(\gamma_{n3}h_2)] \sin(\alpha_n y) e^{-j\beta z}$$

equating the above expressions, we get

$$M_{n3} \cos(\gamma_{n3}h_2) = -M_{n2} \sin(\gamma_{n2}d) + M'_{n2} \cos(\gamma_{n2}d)$$

this can be written as

$$\begin{aligned} & \frac{1}{\alpha_n^2 + \beta^2} [-\alpha_n \gamma_{n3} B_{n3} + \omega \beta \epsilon_0 A_{n3}] \cos(\gamma_{n3} h_2) = \\ & - \frac{1}{\alpha_n^2 + \beta^2} [\alpha_n \gamma_{n2} B_{n2} - \omega \beta \epsilon_0 \epsilon_{r2} A_{n2}] \sin(\gamma_{n2} d) \\ & + \frac{1}{\alpha_n^2 + \beta^2} [-\alpha_n \gamma_{n2} B'_{n2} + \omega \beta \epsilon_0 \epsilon_{r2} A'_{n2}] \cos(\gamma_{n2} d) \end{aligned}$$

on rearranging we get

$$\begin{aligned} & \frac{1}{\alpha_n^2 + \beta^2} [-\alpha_n \gamma_{n3} B_{n3} + \omega \beta \epsilon_0 A_{n3}] = \\ & - \frac{1}{\alpha_n^2 + \beta^2} [\alpha_n \gamma_{n2} B_{n2} - \omega \beta \epsilon_0 \epsilon_{r2} A_{n2}] \frac{\sin(\gamma_{n2} d)}{\cos(\gamma_{n3} h_2)} \\ & + \frac{1}{\alpha_n^2 + \beta^2} [-\alpha_n \gamma_{n2} B'_{n2} + \omega \beta \epsilon_0 \epsilon_{r2} A'_{n2}] \frac{\cos(\gamma_{n2} d)}{\cos(\gamma_{n3} h_2)} \end{aligned} \quad (2.83)$$

Similarly taking expressions for $H_z^{(2)}$ and $H_z^{(3)}$ i. e.

$$H_z^{(2)} = \sum_{n=0}^{\infty} [D_{n2} \sin(\gamma_{n2} x) + D'_{n2} \cos(\gamma_{n2} x)] \cos(\alpha_n y) e^{-j\beta z}$$

$$H_z^{(3)} = \sum_{n=1}^{\infty} D_{n3} \cos(\gamma_{n3} (x + d + h_2)) \cos(\alpha_n y) e^{-j\beta z}$$

at $x = -d$ above expressions become

$$H_z^{(2)} = \sum_{n=0}^{\infty} [D_{n2} \sin(-\gamma_{n2} d) + D'_{n2} \cos(-\gamma_{n2} d)] \cos(\alpha_n y) e^{-j\beta z}$$

$$H_z^{(3)} = \sum_{n=0}^{\infty} [D_{n3} \cos(\gamma_{n3} h_2)] \cos(\alpha_n y) e^{-j\beta z}$$

equating the above expressions, we get

$$D_{n3} \cos(\gamma_{n3} h_2) = -D_{n2} \sin(\gamma_{n2} d) + D'_{n2} \cos(\gamma_{n2} d)$$

this can be written as

$$\begin{aligned} & \frac{1}{\alpha_n^2 + \beta^2} [-j\beta \gamma_{n3} B_{n3} - j\omega \epsilon_0 \alpha_n A_{n3}] \cos(\gamma_{n3} h_2) = \\ & - \frac{1}{\alpha_n^2 + \beta^2} [j\beta \gamma_{n2} B_{n2} - j\omega \epsilon_0 \epsilon_{r2} \alpha_n A_{n2}] \sin(\gamma_{n2} d) \\ & + \frac{1}{\alpha_n^2 + \beta^2} [-j\beta \gamma_{n2} B'_{n2} - j\omega \epsilon_0 \epsilon_{r2} \alpha_n A'_{n2}] \cos(\gamma_{n2} d) \end{aligned}$$

on rearranging we get

$$\begin{aligned}
& \frac{1}{\alpha_n^2 + \beta^2} [-j\beta\gamma_{n3} B_{n3} - j\omega\epsilon_0\alpha_n A_{n3}] = \\
& - \frac{1}{\alpha_n^2 + \beta^2} [j\beta\gamma_{n2} B_{n2} - j\omega\epsilon_0\epsilon_{r2}\alpha_n A_{n2}] \frac{\sin(\gamma_{n2}d)}{\cos(\gamma_{n3}h_2)} \\
& + \frac{1}{\alpha_n^2 + \beta^2} [-j\beta\gamma_{n2} B'_{n2} - j\omega\epsilon_0\epsilon_{r2}\alpha_n A'_{n2}] \frac{\cos(\gamma_{n2}d)}{\cos(\gamma_{n3}h_2)} \quad (2.84)
\end{aligned}$$

On combining equations 2.83 and 2.84 we get

$$\begin{aligned}
& \begin{bmatrix} \beta\omega\epsilon_0\epsilon_{r3} & -\alpha_n\gamma_{n3} \\ -j\omega\epsilon_0\epsilon_{r3}\alpha_n & -j\beta\gamma_{n3} \end{bmatrix} \begin{bmatrix} A_{n3} \\ B_{n3} \end{bmatrix} = \\
& \begin{bmatrix} -\omega\beta\epsilon_0\epsilon_{r2} & -\alpha_n\gamma_{n2} & \omega\beta\epsilon_0\epsilon_{r2} & -\alpha_n\gamma_{n2} \\ j\omega\epsilon_0\epsilon_{r3}\alpha_n & -j\beta\gamma_{n2} & -j\omega\epsilon_0\epsilon_{r2}\alpha_n & -j\beta\gamma_{n2} \end{bmatrix} \begin{bmatrix} A_{n2} \frac{\sin(\gamma_{n2}d)}{\cos(\gamma_{n3}h_2)} \\ B_{n2} \frac{\sin(\gamma_{n2}d)}{\cos(\gamma_{n3}h_2)} \\ A'_{n2} \frac{\cos(\gamma_{n2}d)}{\cos(\gamma_{n3}h_2)} \\ B'_{n2} \frac{\cos(\gamma_{n2}d)}{\cos(\gamma_{n3}h_2)} \end{bmatrix} \quad (2.85)
\end{aligned}$$

Taking the coeff matrix of A_{n3} and B_{n3} to the right hand side of the expression, we get

$$\begin{aligned}
& \begin{bmatrix} A_{n3} \\ B_{n3} \end{bmatrix} = \frac{1}{-j\omega\epsilon_0\epsilon_{r3}\beta^2\gamma_{n3} - j\omega\epsilon_0\epsilon_{r3}\alpha_n^2\gamma_{n3}} \begin{bmatrix} -j\beta\gamma_{n3} & \alpha_n\gamma_{n3} \\ -j\omega\epsilon_0\epsilon_{r3}\alpha_n & \beta\omega\epsilon_0\epsilon_{r3} \end{bmatrix} \times \\
& \begin{bmatrix} -\omega\beta\epsilon_0\epsilon_{r2} & -\alpha_n\gamma_{n2} & \omega\beta\epsilon_0\epsilon_{r2} & -\alpha_n\gamma_{n2} \\ j\omega\epsilon_0\epsilon_{r3}\alpha_n & -j\beta\gamma_{n2} & -j\omega\epsilon_0\epsilon_{r2}\alpha_n & -j\beta\gamma_{n2} \end{bmatrix} \begin{bmatrix} A_{n2} \frac{\sin(\gamma_{n2}d)}{\cos(\gamma_{n3}h_2)} \\ B_{n2} \frac{\sin(\gamma_{n2}d)}{\cos(\gamma_{n3}h_2)} \\ A'_{n2} \frac{\cos(\gamma_{n2}d)}{\cos(\gamma_{n3}h_2)} \\ B'_{n2} \frac{\cos(\gamma_{n2}d)}{\cos(\gamma_{n3}h_2)} \end{bmatrix}
\end{aligned}$$

This can be written as

$$\begin{bmatrix} A_{n_3} \\ B_{n_3} \end{bmatrix} = \frac{1}{-j\omega\epsilon_0\epsilon_{r_3}\gamma_{n_3}p} \times \begin{bmatrix} j\omega\epsilon_0\epsilon_{r_2}\gamma_{n_3}p & 0 & -j\omega\epsilon_0\epsilon_{r_2}\gamma_{n_3}p & 0 \\ 0 & j\omega\epsilon_0\epsilon_{r_3}\gamma_{n_2}p & 0 & j\omega\epsilon_0\epsilon_{r_3}\gamma_{n_2}p \end{bmatrix} \begin{bmatrix} A_{n_2} \frac{\sin(\gamma_{n_2}d)}{\cos(\gamma_{n_3}h_2)} \\ B_{n_2} \frac{\sin(\gamma_{n_2}d)}{\cos(\gamma_{n_3}h_2)} \\ A'_{n_2} \frac{\cos(\gamma_{n_2}d)}{\cos(\gamma_{n_3}h_2)} \\ B'_{n_2} \frac{\cos(\gamma_{n_2}d)}{\cos(\gamma_{n_3}h_2)} \end{bmatrix}$$

where $p=(\alpha_n^2 + \beta^2)$

$$\begin{bmatrix} A_{n_3} \\ B_{n_3} \end{bmatrix} = \begin{bmatrix} \frac{-\epsilon_{r_2}}{\epsilon_{r_3}} & 0 & \frac{\epsilon_{r_2}}{\epsilon_{r_3}} & 0 \\ 0 & \frac{\gamma_{n_2}}{\gamma_{n_3}} & 0 & \frac{\gamma_{n_2}}{\gamma_{n_3}} \end{bmatrix} \times \begin{bmatrix} A_{n_2} \frac{\sin(\gamma_{n_2}d)}{\cos(\gamma_{n_3}h_2)} \\ B_{n_2} \frac{\sin(\gamma_{n_2}d)}{\cos(\gamma_{n_3}h_2)} \\ A'_{n_2} \frac{\cos(\gamma_{n_2}d)}{\cos(\gamma_{n_3}h_2)} \\ B'_{n_2} \frac{\cos(\gamma_{n_2}d)}{\cos(\gamma_{n_3}h_2)} \end{bmatrix} \quad (2.86)$$

On equating and combining 2.82 and 2.86

Expanding and equating expressions for A_{n_3}

$$\frac{-\gamma_{n_2}}{\gamma_{n_3}} \left[A_{n_2} \frac{\cos(\gamma_{n_2}d)}{\sin(\gamma_{n_3}h_2)} \right] + \frac{-\gamma_{n_2}}{\gamma_{n_3}} \left[A'_{n_2} \frac{\sin(\gamma_{n_2}d)}{\sin(\gamma_{n_3}h_2)} \right] = \frac{-\epsilon_{r_2}}{\epsilon_{r_3}} \left[A_{n_2} \frac{\sin(\gamma_{n_2}d)}{\cos(\gamma_{n_3}h_2)} \right] + \frac{\epsilon_{r_2}}{\epsilon_{r_3}} \left[A'_{n_2} \frac{\cos(\gamma_{n_2}d)}{\cos(\gamma_{n_3}h_2)} \right]$$

on rearranging we get

$$A'_{n_2} = A_{n_2} \frac{\left[\frac{-\gamma_{n_2} \cos(\gamma_{n_2}d)}{\gamma_{n_3} \sin(\gamma_{n_3}h_2)} \right] + \left[\frac{\epsilon_{r_2} \sin(\gamma_{n_2}d)}{\epsilon_{r_3} \cos(\gamma_{n_3}h_2)} \right]}{\left[\frac{\epsilon_{r_2} \cos(\gamma_{n_2}d)}{\epsilon_{r_3} \cos(\gamma_{n_3}h_2)} \right] + \left[\frac{\gamma_{n_2} \sin(\gamma_{n_2}d)}{\gamma_{n_3} \sin(\gamma_{n_3}h_2)} \right]}$$

this simplifies to

$$A'_{n_2} = A_{n_2} F_1$$

where

$$F_1 = \left[\frac{-\gamma_{n_2} \epsilon_{r_3} \cos(\gamma_{n_2}d) \cos(\gamma_{n_3}h_2) + \gamma_{n_3} \epsilon_{r_2} \sin(\gamma_{n_2}d) \sin(\gamma_{n_3}h_2)}{\gamma_{n_3} \epsilon_{r_2} \cos(\gamma_{n_2}d) \sin(\gamma_{n_3}h_2) + \gamma_{n_2} \epsilon_{r_3} \sin(\gamma_{n_2}d) \cos(\gamma_{n_3}h_2)} \right]$$

Expanding and equating expressions for B_{n_3}

$$\left[B_{n_2} \frac{\cos(\gamma_{n_2}d)}{\sin(\gamma_{n_3}h_2)} \right] + \left[-B'_{n_2} \frac{\sin(\gamma_{n_2}d)}{\sin(\gamma_{n_3}h_2)} \right] = \frac{\gamma_{n_2}}{\gamma_{n_3}} \left[B_{n_2} \frac{\sin(\gamma_{n_2}d)}{\cos(\gamma_{n_3}h_2)} \right] + \frac{\gamma_{n_2}}{\gamma_{n_3}} \left[B'_{n_2} \frac{\cos(\gamma_{n_2}d)}{\cos(\gamma_{n_3}h_2)} \right]$$

on rearranging we get

$$B'_{n_2} = B_{n_2} \left[\frac{\left[\frac{\cos(\gamma_{n_2} d)}{\sin(\gamma_{n_3} h_2)} \right] - \left[\frac{\gamma_{n_2} \sin(\gamma_{n_2} d)}{\gamma_{n_3} \cos(\gamma_{n_3} h_2)} \right]}{\left[\frac{\gamma_{n_2} \cos(\gamma_{n_2} d)}{\gamma_{n_3} \cos(\gamma_{n_3} h_2)} \right] + \left[\frac{\sin(\gamma_{n_2} d)}{\sin(\gamma_{n_3} h_2)} \right]} \right]$$

this simplifies to

$$B'_{n_2} = B_{n_2} F_2$$

where

$$F_2 = \left[\frac{\gamma_{n_3} \cos(\gamma_{n_2} d) \cos(\gamma_{n_3} h_2) - \gamma_{n_2} \sin(\gamma_{n_2} d) \sin(\gamma_{n_3} h_2)}{\gamma_{n_2} \cos(\gamma_{n_2} d) \sin(\gamma_{n_3} h_2) + \gamma_{n_3} \sin(\gamma_{n_2} d) \cos(\gamma_{n_3} h_2)} \right]$$

2.6 Boundary Conditions at the plane of strip Conductor

At $x = 0$

$$H_y^{(1)} - H_y^{(2)} = I_z(y) \quad (2.87)$$

from this we get

$$\begin{aligned} & \sum_{n=1}^{\infty} M_{n_1} \cos(\gamma_{n_1} (x - h_1)) \sin(\alpha_n y) e^{-j\beta z} - \\ & \sum_{n=1}^{\infty} [M_{n_2} \sin(\gamma_{n_2} x) + M'_{n_2} \cos(\gamma_{n_2} x)] \sin(\alpha_n y) e^{-j\beta z} = I_z(y) \end{aligned}$$

On substituting $x = 0$

$$\sum_{n=1}^{\infty} (M_{n_1} \cos(\gamma_{n_1} h_1) - M'_{n_2}) \sin(\alpha_n y) = I_z(y) \quad (2.88)$$

Multiplying both sides with $\sin(\alpha_n y)$ and on integrating from 0 to b i. e. applying orthogonality condition we get

$$\begin{aligned} \int_0^b \sum_{n=1}^{\infty} (M_{n_1} \cos(\gamma_{n_1} h_1) - M'_{n_2}) \sin(\alpha_n y) \sin(\alpha_n y) dy &= \int_0^b I_z(y) \sin(\alpha_n y) dy \\ M_{n_1} \cos(\gamma_{n_1} h_1) - M'_{n_2} &= \frac{y_n}{b} L_{1n} \end{aligned}$$

where

$$L_{1n} = \int_0^b I_z(y) \sin(\alpha_n y) dy$$

Expanding the above expression, we get

$$\frac{1}{\alpha_n^2 + \beta^2} [-\alpha_n B_{n_1} \gamma_{n_1} + \omega \beta \epsilon_0 A_{n_1}] \cos(\gamma_{n_1} h_1) - \frac{1}{\alpha_n^2 + \beta^2} [-\alpha_n \gamma_{n_2} B'_{n_2} + \omega \beta \epsilon_0 \epsilon_{r_2} A'_{n_2}] = \frac{q_n}{b} L_{1n}$$

Now on substituting the values of A_{n_2} , A'_{n_2} , B_{n_2} and B'_{n_2}

$$\begin{aligned} A'_{n_2} &= A_{n_2} F_1 \\ B'_{n_2} &= B_{n_2} F_2 \\ A_{n_2} &= -A_{n_1} \frac{\gamma_{n_1}}{\gamma_{n_2}} \sin(\gamma_{n_1} h_1) \\ B_{n_2} &= -B_{n_1} \sin(\gamma_{n_1} h_1) \end{aligned}$$

we get

$$\begin{aligned} & [\omega \beta \epsilon_0 A_{n_1} [\cos(\gamma_{n_1} h_1) - \epsilon_{r_2} \frac{\gamma_{n_1}}{\gamma_{n_2}} \sin(\gamma_{n_1} h_1) F_1]] \\ & + B_{n_1} \alpha_n [-\gamma_{n_1} \cos(\gamma_{n_1} h_1) - \gamma_{n_2} \sin(\gamma_{n_1} h_1) F_2] = \frac{q_n}{b} L_{1n} (\alpha_n^2 + \beta^2) \end{aligned} \quad (2.89)$$

Similarly we have

At $x = 0$

$$H_z^{(1)} - H_z^{(2)} = I_y(y) \quad (2.90)$$

Or

$$\begin{aligned} & \sum_{n=1}^{\infty} D_{n_1} \cos(\gamma_{n_1} (x - h_1)) \cos(\alpha_n y) e^{-\beta z} \\ & - \sum_{n=0}^{\infty} [D_{n_2} \sin(\gamma_{n_2} x) + D'_{n_2} \cos(\gamma_{n_2} x)] \cos(\alpha_n y) e^{-\beta z} = I_y(y) \end{aligned}$$

On substituting $x = 0$, we get

$$\sum_{n=0}^{\infty} (D_{n_1} \cos(\gamma_{n_1} h_1) - D'_{n_2}) \cos(\alpha_n y) = I_y(y) \quad (2.91)$$

multiplying both sides with $\cos(\alpha_n y)$ and on integrating from 0 to b i. e. applying orthogonality condition we get

$$\begin{aligned} \int_0^b \sum_{n=0}^{\infty} (D_{n_1} \cos(\gamma_{n_1} h_1) - D'_{n_2}) \cos(\alpha_n y) \cos(\alpha_n y) dy &= \int_0^b I_y(y) \cos(\alpha_n y) dy \\ D_{n_1} \cos(\gamma_{n_1} h_1) - D'_{n_2} &= \frac{q_n}{b} L_{2n} \end{aligned}$$

where

$$L_{2n} = \int_0^b I_y(y) \cos(\alpha_n y) dy$$

On expanding, above expression, we get

$$\begin{aligned} \frac{1}{\alpha_n^2 + \beta^2} [-j\beta\gamma_{n1} B_{n1} - j\omega\epsilon_0\alpha_n A_{n1}] \cos(\gamma_{n1} h_1) - \\ \frac{1}{\alpha_n^2 + \beta^2} [-j\beta\gamma_{n2} B'_{n2} - j\omega\epsilon_0\epsilon_{r2}\alpha_n A'_{n2}] = \frac{\gamma_{n1}}{b} L_{2n} \end{aligned}$$

substituting the values of A_{n2} , A'_{n2} , B_{n2} , and B'_{n2}

$$\begin{aligned} A'_{n2} &= A_{n2} F_1 \\ B'_{n2} &= B_{n2} F_2 \\ A_{n2} &= -A_{n1} \frac{\gamma_{n1}}{\gamma_{n2}} \sin(\gamma_{n1} h_1) \\ B_{n2} &= -B_{n1} \sin(\gamma_{n1} h_1) \end{aligned}$$

$$\begin{aligned} [j\omega\alpha_n\epsilon_0 A_{n1} [\cos(\gamma_{n1} h_1) - \epsilon_{r2} \frac{\gamma_{n1}}{\gamma_{n2}} \sin(\gamma_{n1} h_1) F_1]] \\ + j\beta B_{n1} [\gamma_{n1} \cos(\gamma_{n1} h_1) + \gamma_{n2} \sin(\gamma_{n1} h_1) F_2] = \frac{\gamma_{n1}}{b} L_{2n} (\alpha_n^2 + \beta^2) \end{aligned} \quad (2.92)$$

Let

$$[\cos(\gamma_{n1} h_1) - \epsilon_{r2} \frac{\gamma_{n1}}{\gamma_{n2}} \sin(\gamma_{n1} h_1) F_1] = F_{11}$$

$$[\gamma_{n1} \cos(\gamma_{n1} h_1) + \gamma_{n2} \sin(\gamma_{n1} h_1) F_2] = F_{22}$$

we can make these substitutions in equations 2.89 and 2.92.

They now become

$$\omega\beta\epsilon_0 A_{n1} F_{11} - B_{n1} \alpha_n F_{22} = \frac{\gamma_{n1}}{b} L_{1n} (\alpha_n^2 + \beta^2) \quad (2.93)$$

$$j\omega\alpha_n\epsilon_0 A_{n1} F_{11} + j\beta B_{n1} F_{22} = \frac{\gamma_{n1}}{b} L_{2n} (\alpha_n^2 + \beta^2) \quad (2.94)$$

These two, are equations in A_{n_1} and B_{n_1} . We can now solve for A_{n_1} and B_{n_1} .

Solving for A_{n_1} .

On multiplying 2.93 with β , 2.94 with $j\alpha_n$ and adding we get

$$\omega\epsilon_0 A_{n_1} F_{11}(\alpha_n^2 + \beta^2) = (\alpha_n^2 + \beta^2) \left[\frac{q_n}{b} \beta L_{1n} + j\alpha_n \frac{p_n}{b} L_{2n} \right]$$

On rearranging we get

$$A_{n_1} = \frac{1}{b\omega\epsilon_0 F_{11}} [\beta q_n L_{1n} - j\alpha_n p_n L_{2n}] \quad (2.95)$$

Solving for B_{n_1} .

On multiplying 2.93 with α_n , 2.94 with $j\beta$ and adding we get

$$-B_{n_1} F_{22}(\alpha_n^2 + \beta^2) = (\alpha_n^2 + \beta^2) \left[\frac{q_n}{b} \alpha_n L_{1n} + j\beta \frac{p_n}{b} L_{2n} \right]$$

On rearranging we get

$$B_{n_1} = -\frac{1}{bF_{22}} [\alpha_n q_n L_{1n} + j\beta p_n L_{2n}] \quad (2.96)$$

Also at $x = 0$ we can now determine $E_y^{(1)}$ and $E_z^{(1)}$ as under we have

$$E_y^{(1)} = \sum_{n=0}^{\infty} S_{n_1} \sin(\gamma_{n_1}(x - h_1)) \cos(\alpha_n y) e^{-j\beta z}$$

$$E_z^{(1)} = \sum_{n=1}^{\infty} C_{n_1} \sin(\gamma_{n_1}(x - h_1)) \sin(\alpha_n y) e^{-j\beta z}$$

at $x = 0$ above expressions become

$$-\sum_{n=0}^{\infty} S_{n_1} \sin(\gamma_{n_1} h_1) \cos(\alpha_n y) = E_y(y) \quad (2.97)$$

$$-\sum_{n=1}^{\infty} C_{n_1} \sin(\gamma_{n_1} h_1) \sin(\alpha_n y) = E_z(y) \quad (2.98)$$

$$\text{we have } S_{n_1} = \frac{1}{\alpha_n^2 + \beta^2} [-\alpha_n A_{n_1} \gamma_{n_1} - \omega\beta\mu_0 B_{n_1}]$$

On substituting the value of A_{n_1} and B_{n_1} from eqn 2.95 and 2.96 in the above expression for S_{n_1} we get

$$S_{n_1} = \frac{1}{b(\alpha_n^2 + \beta^2)} \left[p_n L_{2n} \left[\frac{j\alpha_n^2 \gamma_{n_1}}{\omega\epsilon_0 F_{11}} + \frac{j\omega\beta^2 \mu_0}{F_{22}} \right] + q_n L_{1n} \left[\frac{\beta\omega\mu_0 \alpha_n}{F_{22}} - \frac{\alpha_n \beta \gamma_{n_1}}{\omega\epsilon_0 F_{11}} \right] \right]$$

$$\text{Similarly we have } C_{n_1} = \frac{1}{\alpha_n^2 + \beta^2} [j\beta A_{n_1} \gamma_{n_1} - j\omega\mu_0 \alpha_n B_{n_1}]$$

On substituting the value of A_{n_1} and B_{n_1} from eqn 2.95 and 2.96 in the above expression for C_{n_1} we get

$$C_{n_1} = \frac{1}{b(\alpha_n^2 + \beta^2)} \left[p_n L_{2n} \left[\frac{\beta \alpha_n \gamma_{n_1}}{\omega \epsilon_0 I'_{11}} - \frac{\omega \beta \mu_0 \alpha_n}{I'_{22}} \right] + q_n L_{1n} \left[\frac{j \beta^2 \gamma_{n_1}}{\omega \epsilon_0 I'_{11}} + \frac{j \omega \mu_0 \alpha_n^2}{b I'_{22}} \right] \right]$$

Substituting above expanded values of S_{n_1} and C_{n_1} in equations 2.97 and 2.98 we get

$$\sum_{n=1}^{\infty} p_n G_{11} L_{2n} \sin(\alpha_n y) + \sum_{n=1}^{\infty} q_n L_{1n} G_{12} \sin(\alpha_n y) = E_z(y) \quad (2.99)$$

$$\sum_{n=0}^{\infty} p_n G_{21} L_{2n} \cos(\alpha_n y) + \sum_{n=0}^{\infty} q_n L_{1n} G_{22} \cos(\alpha_n y) = E_y(y) \quad (2.100)$$

where

$$\begin{aligned} G_{11} &= \frac{- \left[\left[\frac{\beta \alpha_n \gamma_{n_1}}{\omega \epsilon_0 I'_{11}} - \frac{\omega \beta \mu_0 \alpha_n}{I'_{22}} \right] \sin(\gamma_{n_1} h_1) \right]}{b(\alpha_n^2 + \beta^2)} \\ G_{12} &= \frac{- \left[\left[\frac{j \beta^2 \gamma_{n_1}}{\omega \epsilon_0 I'_{11}} + \frac{j \omega \mu_0 \alpha_n^2}{I'_{22}} \right] \sin(\gamma_{n_1} h_1) \right]}{b(\alpha_n^2 + \beta^2)} \\ G_{21} &= \frac{- \left[\left[\frac{j \alpha_n^2 \gamma_{n_1}}{\omega \epsilon_0 I'_{11}} + \frac{j \omega \beta^2 \mu_0}{I'_{22}} \right] \sin(\gamma_{n_1} h_1) \right]}{b(\alpha_n^2 + \beta^2)} \\ G_{22} &= \frac{- \left[\left[\frac{\beta \omega \mu_0 \alpha_n}{I'_{22}} - \frac{\alpha_n \beta \gamma_{n_1}}{\omega \epsilon_0 I'_{11}} \right] \sin(\gamma_{n_1} h_1) \right]}{b(\alpha_n^2 + \beta^2)} \end{aligned}$$

2.7 Dispersion equations

We take the expressions for L_{1n} and L_{2n}

$$L_{1n} = \int_0^b I_z(y) \sin(\alpha_n y) dy$$

$$L_{2n} = \int_0^b I_y(y) \cos(\alpha_n y) dy,$$

these can be expanded as an infinite summation in terms of suitably chosen basis functions as under:

$$I_z(y) = \sum_{k=1}^{\infty} c_k I_z^k(y) \quad (2.101)$$

$$I_y(y) = \sum_{k=1}^{\infty} d_k I_y^k(y) \quad (2.102)$$

On substituting the expanded expressions we get the following expressions

$$L_{1n} = \int_0^b \sum_{k=1}^{\infty} c_k I_z^k(y) \sin(\alpha_n y) dy$$

$$L_{2n} = \int_0^b \sum_{k=1}^{\infty} d_k I_y^k(y) \cos(\alpha_n y) dy$$

Or

$$L_{1n} = \sum_{k=1}^{\infty} c_k \int_0^b I_z^k(y) \sin(\alpha_n y) dy$$

$$L_{2n} = \sum_{k=1}^{\infty} d_k \int_0^b I_y^k(y) \cos(\alpha_n y) dy$$

These can also be written as

$$L_{1n} = \sum_{k=1}^{\infty} c_k L_{1n}^k \quad (2.103)$$

$$L_{2n} = \sum_{k=1}^{\infty} d_k L_{2n}^k \quad (2.104)$$

where

$$L_{1n}^k = \int_0^b I_z^k(y) \sin(\alpha_n y) dy$$

$$L_{2n}^k = \int_0^b I_y^k(y) \cos(\alpha_n y) dy$$

Substituting equations 2.103 and 2.104 in

$$\sum_{n=1}^{\infty} p_n G_{11} L_{2n} \sin(\alpha_n y) + \sum_{n=1}^{\infty} q_n L_{1n} G_{12} \sin(\alpha_n y) = E_z(y)$$

$$\sum_{n=0}^{\infty} p_n G_{21} L_{2n} \cos(\alpha_n y) + \sum_{n=0}^{\infty} q_n L_{1n} G_{22} \cos(\alpha_n y) = E_y(y)$$

we get

$$\sum_{k=1}^{\infty} d_k \sum_{n=1}^{\infty} p_n G_{11} L_{2n}^k \sin(\alpha_n y) + \sum_{k=1}^{\infty} c_k \sum_{n=1}^{\infty} q_n L_{1n}^k G_{12} \sin(\alpha_n y) = E_z(y) \quad (2.105)$$

$$\sum_{k=1}^{\infty} d_k \sum_{n=0}^{\infty} p_n G_{21} L_{2n}^k \cos(\alpha_n y) + \sum_{k=1}^{\infty} c_k \sum_{n=0}^{\infty} q_n L_{1n}^k G_{22} \cos(\alpha_n y) = E_y(y) \quad (2.106)$$

We now define the inner product as

$$\langle f(x), g(x) \rangle = \int_0^b f(x) g(x) dx$$

Taking inner product of equations 2.105 and 2.106 with $I_z^k(y)$ and $I_y^k(y)$ respectively and noting $I_z^k(y)$ and $E_z(y)$, $I_y^k(y)$ and $E_y(y)$ pairs are nonzero in complementary regions,

we now get

$$\sum_{k=1}^{\infty} d_k \sum_{n=1}^{\infty} p_n G_{11} L_{2n}^k L_{1n}^k + \sum_{k=1}^{\infty} c_k \sum_{n=1}^{\infty} q_n G_{12} L_{1n}^k L_{1n}^k = 0 \quad (2.107)$$

$$\sum_{k=1}^{\infty} d_k \sum_{n=0}^{\infty} p_n G_{21} L_{2n}^k L_{2n}^k + \sum_{k=1}^{\infty} c_k \sum_{n=1}^{\infty} q_n G_{22} L_{1n}^k L_{2n}^k = 0 \quad (2.108)$$

For this problem now we make a suitable choice of basis functions. These one term expansions satisfy the edge conditions at $|x| = \frac{w}{2}$ as shown in the figure 2.2.

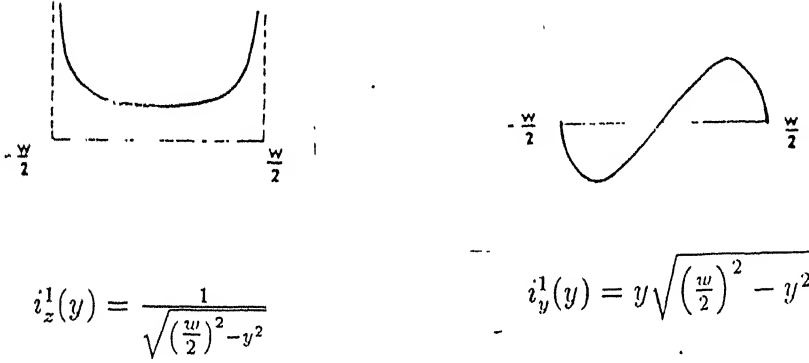


Figure 2.2: Qualified one term basis function satisfying edge condition at $|x| = (\frac{w}{2})$.

where

$$i_z^1(y) = \frac{1}{\sqrt{\left(\frac{w}{2}\right)^2 - y^2}}$$

$$i_y^1(y) = y \sqrt{\left(\frac{w}{2}\right)^2 - y^2}$$

Such a choice now fixes $k = 1$, thus equations 2.107 and 2.108 can be combined as under

$$\begin{bmatrix} A & B \\ C & D \end{bmatrix} \begin{bmatrix} c_k \\ d_k \end{bmatrix} = 0 \quad (2.109)$$

where

$$A = \sum_{n=1}^{\infty} q_n G_{12} L_{1n}^{-1} L_{1n}^{-1}$$

$$B = \sum_{n=1}^{\infty} p_n G_{11} L_{2n}^{-1} L_{1n}^{-1}$$

$$C = \sum_{n=1}^{\infty} q_n G_{22} L_{1n}^{-1} L_{2n}^{-1}$$

$$D = \sum_{n=1}^{\infty} p_n G_{21} L_{2n}^{-1} L_{2n}^{-1}$$

The integrals can be completely solved by using the identity given in [12]. The integrals evaluate as under

for $\alpha_n \neq 0$

$$L_{1n}^{-1} = \pi J_0(\alpha_n \frac{w}{2}) \sin(\alpha_n \frac{w}{2})$$

$$L_{2n}^{-1} = (-\sin(\alpha_n \frac{b}{2})) \left[(\frac{w}{2})^2 \pi \left[\frac{2J_1(\alpha_n \frac{w}{2}) - (\alpha_n \frac{w}{2}) J_0(\alpha_n \frac{w}{2})}{(\alpha_n \frac{w}{2})^2} \right] \right]$$

$$L_{1n}^{-1} = L_{2n}^{-1} = 0 \text{ for } \alpha_n = 0$$

The determinant of the coefficient matrix when equated to zero

$$AD - BC = 0$$

yields an equation in terms of β .

Now, one possible choice of definition of characteristic impedance is

$$Z_0 = \frac{2P_{av}}{I^2} \quad (2.110)$$

where

$$I = \int_0^b I_z(y) dy \quad (2.111)$$

In above expressions P_{av} is time average Poynting power along z axis and I is effective current along the z axis on the strip.

$$P_{av} = \frac{1}{2} \int \int_{reg1 + reg2 + reg3} [E_x H_y^* - E_y H_x^*] dx dy \quad (2.112)$$

this can also be written as

$$P_{av} = \frac{1}{2} [I_1 + I_2 + I_3]$$

Here I_1 , I_2 and I_3 are the integrals over each of the regions 1, 2 and 3.

These can evaluated as under:

$$I_1 = \int_0^b \int_0^{h_1} [E_x^{(1)} H_y^{(1)*} - E_y^{(1)} H_x^{(1)*}] dx dy \quad (2.113)$$

$$I_1 = \sum_{n=0}^{\infty} \frac{b}{4} [(A_{n_1} M_{n_1}^* - S_{n_1} B_{n_1}^*) h_1 + (A_{n_1} M_{n_1}^* + S_{n_1} B_{n_1}^*) \frac{\sin(2\gamma_{n_1} h_1)}{2\gamma_{n_1}}] \quad (2.114)$$

$$I_2 = \int_0^b \int_{-d}^0 [E_x^{(2)} H_y^{(2)*} - E_y^{(2)} H_x^{(2)*}] dx dy \quad (2.115)$$

$$I_2 = \sum_{n=0}^{\infty} \frac{b}{4} \times [[(A'_{n_2} M_{n_2}^{*'} + A_{n_2} M_{n_1}^*) + (B_{n_2}^* S_{n_2} + S'_{n_2} B_{n_2}^{*'})]d + [(A'_{n_2} M_{n_2}^{*'} - A_{n_2} M_{n_2}^*) - (B_{n_2}^* S_{n_2} - S'_{n_2} B_{n_2}^{*'}) \frac{\sin(2\gamma_{n_2} d)}{2\gamma_{n_2}}], \quad (2.116)$$

$$-[(A_{n_2} M_{n_2}^{*'} + A'_{n_2} M_{n_2}^*) - (B_{n_2}^* S'_{n_2} + S_{n_2} B_{n_2}^{*'}) \frac{\sin(2\gamma_{n_2} d)}{\gamma_{n_2}}]] \quad (2.117)$$

$$I_3 = \int_0^b \int_{-h_2-d}^{-d} [E_x^{(3)} H_y^{(3)*} - E_y^{(3)} H_x^{(3)*}] dx dy \quad (2.118)$$

$$I_3 = \sum_{n=0}^{\infty} \frac{b}{4} [(A_{n_3} M_{n_3}^* - S_{n_3} B_{n_3}^*) h_2 + (A_{n_3} M_{n_3}^* + S_{n_3} B_{n_3}^*) \frac{\sin(2\gamma_{n_3} h_2)}{2\gamma_{n_3}}] \quad (2.119)$$

This information has been made use of, in the design of the filter and mixer, as enumerated in subsequent pages.

Chapter 3

MIXER DESIGN PRINCIPLES & PHILOSOPHY

3.1 Dielectric Resonators

The DR is made of a low loss, temperature stable, high permittivity, and high-Q ceramic material. It is usually used in regular geometrical shapes like solid cylinder, disc or pill box, tubular, spherical or parrallelopiped. Dimensions and shielding conditions determine the mode of resonance and resonant frequency of the DR. It's small size, and excellent integrability in MICs have made its use very popular in active and passive microwave components. The dimensions of a dielectric resonator are much smaller than those of an empty metallic cavity resonator, resonant at the same frequency by a factor of approximately $\frac{1}{\sqrt{\epsilon_r}}$. If ϵ_r is high, the electric and magnetic fields are confined in and near the resonator, thus having small radiation losses. The unloaded quality factor Q_u is thus improved for low losses in the dielectric resonators. To a first approximation, a DR is considered as the dual of a metallic cavity. The radiation losses of the DR with commonly used permittivities are much greater than the energy losses in the metallic cavities, this makes proper shielding of the dielectric resonator a necessity.

A commonly used resonant mode in the disc shaped DR is $TE_{01\delta}$ mode. The magnetic field lines are contained in the plane parallel to z axis, while the electric field lines are concentric circles around the z axis as shown in the fig 3.1. When the ϵ_r is around 40, more than 95% of the stored electric energy of the $TE_{01\delta}$ mode and more than 60% of the stored magnetic energy are located within the cylinder. The remaining energy is distributed around the resonator, decaying rapidly with distance away from the resonator surface.

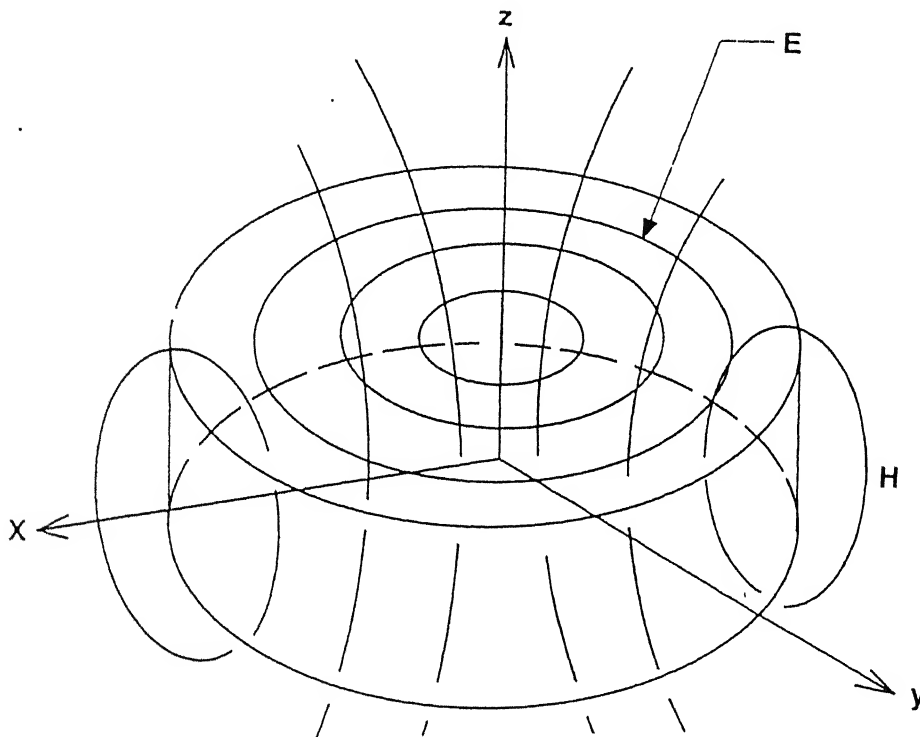


Figure 3.1: Field lines of the resonant mode $TE_{01\delta}$ in a DR

The important properties of the ceramic material to be used for DR's are

- the Q factor,
- temperature coefficient of resonant frequency T_f ,
- the dielectric constant ϵ_r

The Q , T_f and ϵ_r values required for various applications differ, and in general, a proper combination can be achieved by choosing an appropriate material and com-

<i>Composition</i>	ϵ_r	$Q @ 10 \text{ GHz}$	T_f	<i>Freq Range</i>
$Ba_2Ti_9O_{20}$	40	4000	+2	1 to 50 GHz
$BaTi_4O_9$	39	3500	+4	1 to 50 GHz
$(Zr - Sn)TiO_4$	38	4000	-4 to -10	1 to 60 GHz
$Ba(\underset{3}{Zn}_1\underset{3}{Ta}_2)O_2$	29	10000	0 to 10	5 to 60 GHz
$(Ba, Pb)Nd_2Ti_5O_{14}$	90	5000 @ 1 GHz	0 to 6	0.8 to 4 GHz

Table 3.1: Properties of Dielectric Resonators.

position. A number of material compositions have been tried in attempts to develop suitable dielectric materials. These include ceramic mixtures containing TiO_2 , various titanates and zirconates, glass ceramics and alumina based ceramics [4, 5]. Table 3.1 [4] compares different materials developed commercially.

In low dielectric constant materials, the performance is sensitive to shielding due to increase in fields outside the isolated resonator. The temperature coefficient of the resonant frequency T_f can be controlled in some materials by modifying the composition. The Q_u factor of the dielectric resonator decreases with the increase in the frequency. Typically the product $f_0 \times Q_0$ where f_0 is in GHz remains constant. Losses due to housing walls, dielectrics, and adhesives used to support the resonators typically reduce the Q_u by 10% to 20%. A higher Q material is preferred for lower noise oscillations as well as for sharp tuned filters, and lower Q material is preferred for frequency tunable wider band components.

3.1.1 Resonant frequency

The resonant frequency of a resonator is determined by its dimensions and surroundings. Though the geometrical form of a DR is extremely simple, an exact solution of

the Maxwell equations is considerably involved. For this reason, the exact resonant frequency of a particular resonant mode, such as $TE_{01\delta}$, can only be computed by rigorous numerical procedures. Kajfez [6] has presented an approximate solution of the equations involved which yield results with $\pm 2\%$ accuracy. P. Bhartia [4] also gives a set of equations to calculate the resonant frequency of a DR with known dimensions. A set of relations giving variation of resonant frequency with the height of top plate in MIC environment can also be found in [4]. For an isolated resonator, the resonant frequency in GHz is given by the following expression:

$$f_r = \frac{34}{a\epsilon_r} \left[\frac{a}{H} + 3.45 \right] \quad (3.1)$$

3.1.2 Electromagnetic Field Coupling of a DR in MIC Configuration

Depending upon the applications, the dielectric resonator is used in a number of different configurations. In each of these arrangements, it is placed in close proximity with other circuit elements so as to provide electromagnetic field coupling between them. For effective design, it is necessary to have an accurate knowledge of the coupling between the resonator and other circuit elements. The $TE_{01\delta}$ and $TM_{01\delta}$ are most commonly used modes, which can be easily excited in dielectric resonator using microstrip lines, finline, magnetic loop, metallic and dielectric waveguide [5]. Most commonly used configuration of a cylindrical dielectric resonator is, $TE_{01\delta}$ mode coupling with a microstrip line.

Alongside a microstrip line, a DR is incorporated within a microwave circuit by placing it on top of the microstrip substrate as shown in Figure 3.2.

As seen from this figure, the transmission characteristics of the microstrip line in the vicinity of DR get altered by the magnetic field effect. The electric field effect

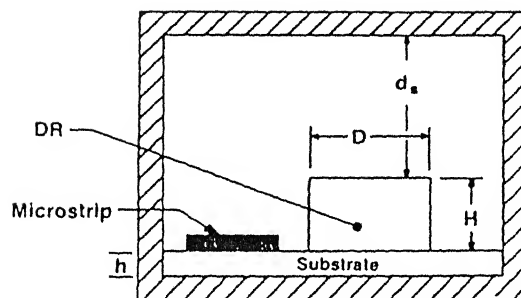


Figure 3.2: DR and microstrip line in MIC environment

as discussed earlier, can be assumed to be very small since most of the electric field of the microstrip line is concentrated under the microstrip line and is orthogonal to the electric field of the resonator. Linking of the magnetic field lines is an interaction between the magnetic field of the resonator and the magnetic field due to the current in the microstrip line. Under the assumptions that presence of microstrip line does not appreciably disturb the field, the DR can be represented by a conducting loop having in series an inductance L_r , a capacitance C_r and a resistance R_r , only TEM mode is carried in the microstrip line and only $TE_{01\delta}$ mode is excited in the resonator and coupling takes place through distributed mutual inductance,

Guillion [6] gives an approximate analysis. It shows that coupling between the microstrip line and resonator depends on the lateral distance between the two, the degree of coupling can be varied by varying this distance. Termination of the microstrip conductor and shielding also influence the performance appreciably. In above analysis [6, 8] a DR coupled to a microstrip line can be represented by a simple parallel tuned

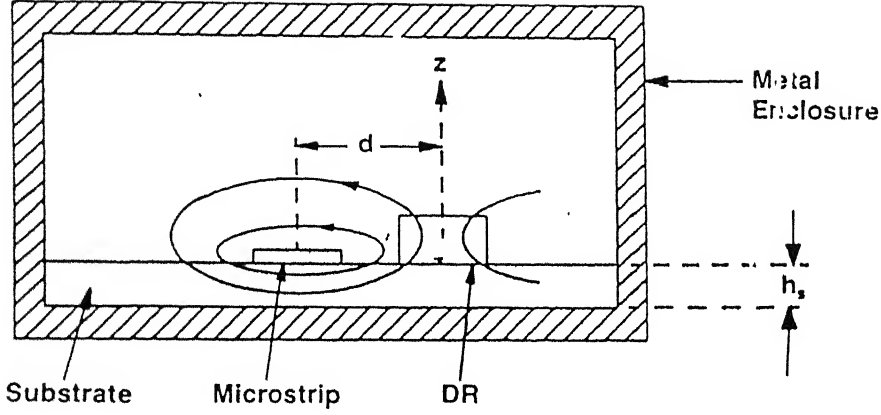


Figure 3.3: DR coupled to microstrip transmission line

circuit as shown in fig. 3.4 where L , C , R are obtained as:

$$L = \frac{L_m^2}{L_r}$$

$$C = \frac{L_r}{L_m^2 \omega_0^2}$$

$$R = \frac{\omega_0 Q_u L_m^2}{L_r}$$

The essence of the problem lies in finding the expression for the quantity $\frac{L_r}{L_m^2}$ in terms of distance between resonator and microstrip. A very good agreement exists between results obtained by Jain [8] and experimental data available in [9, 10] hence these results could be used for practical design.

3.1.3 Coupling between two DRs

Design of a filter using DR involves input/output coupling and interstage coupling information. Previous section dwelled on the input and output coupling between the

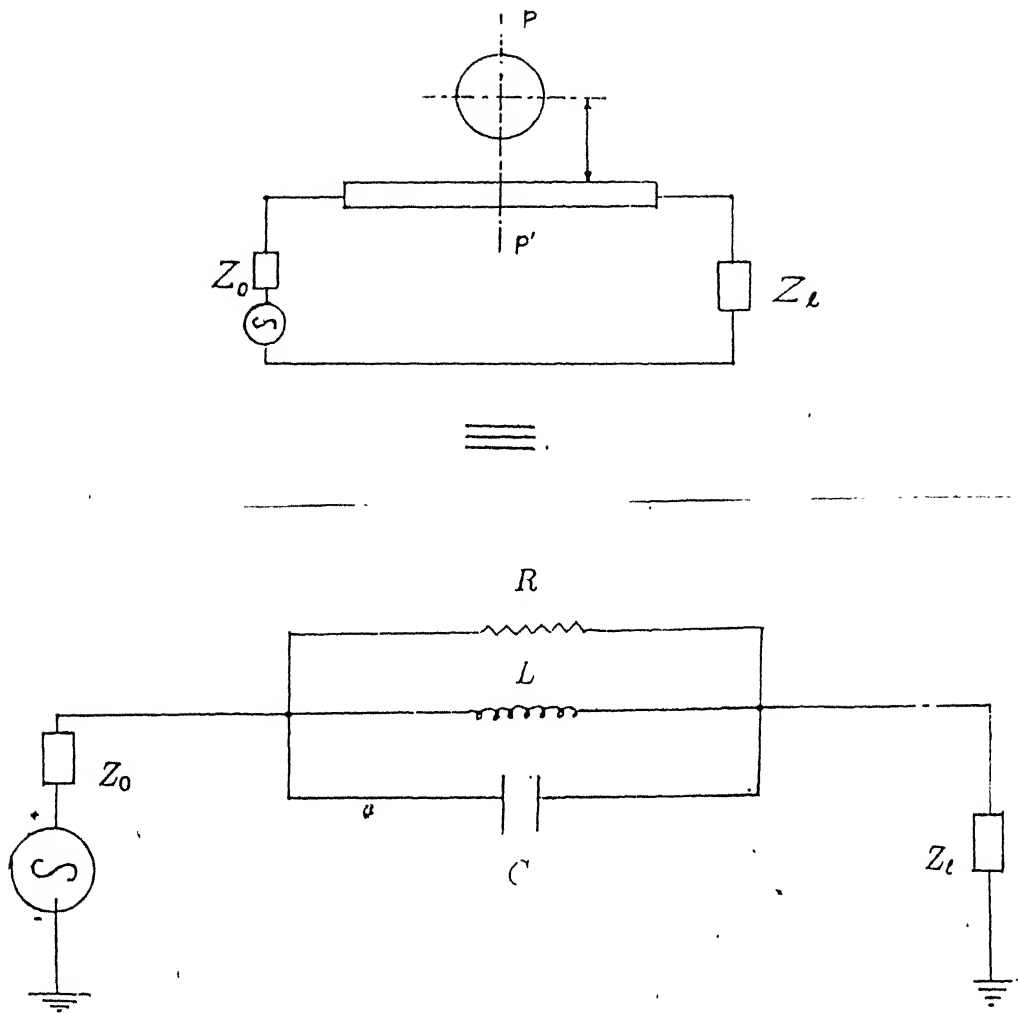


Figure 3.4: Modelling of DR - Microstrip line coupling.

microstrip line and a DR. In this section interstage coupling has been discussed. Interstage coupling provides transfer of energy from one resonator to another resonator either directly or through another transmission line. In [8] coupling coefficient between two identical cylindrical resonators has been derived in terms of the physical and electrical parameters of the resonators, centre to centre spacing between them and dimensions of the surrounding structure. Two or more cylindrical resonators may be coupled directly by placing them over a microstrip substrate adjacent to each other as shown in fig. 3.5.

Lateral distance d between them controls the degree of coupling. Such a type of

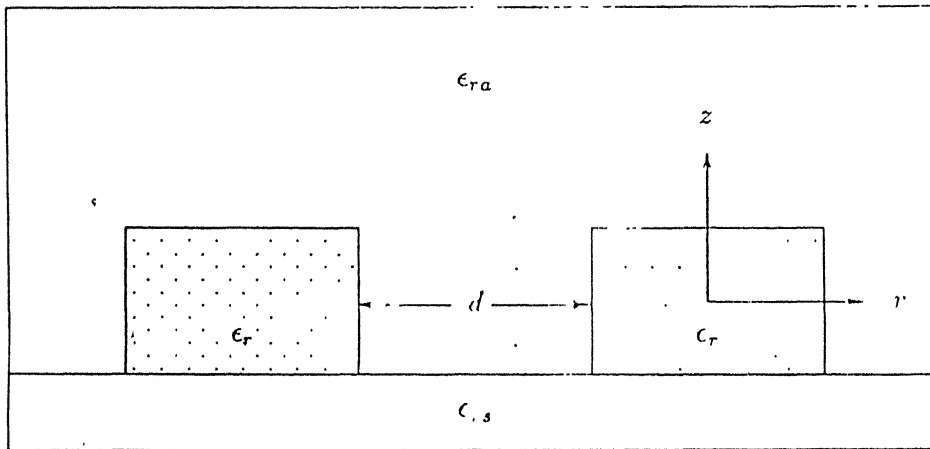


Figure 3.5: Coupled DRs

coupling arrangement is ideal for fabrication. Design graphs showing the mode chart for cylindrical DRs, external quality factor Q_{ext} and coupling coefficient k have been shown in fig. 3.6 through 3.8.

3.1.4 Frequency Tuning

Frequency tuning arrangements are desirable in any DR based microwave circuit. This can be accomplished by electrical or mechanical means.

Electrically, the frequency tuning can be achieved by following, one of the different methods like varactor tuning, ferrite tuning, bias tuning and optical tuning.

For mechanical tuning, use is made of the fact that resonant frequency of the DR in MIC environment is highly sensitive to the shielding (proximity to the ground plane). A tuning screw inserted from the top cover of the package right above the DR can effectively vary the resonant frequency by $\pm 2\%$. Fig. 3.9 shows such an arrangement [4].

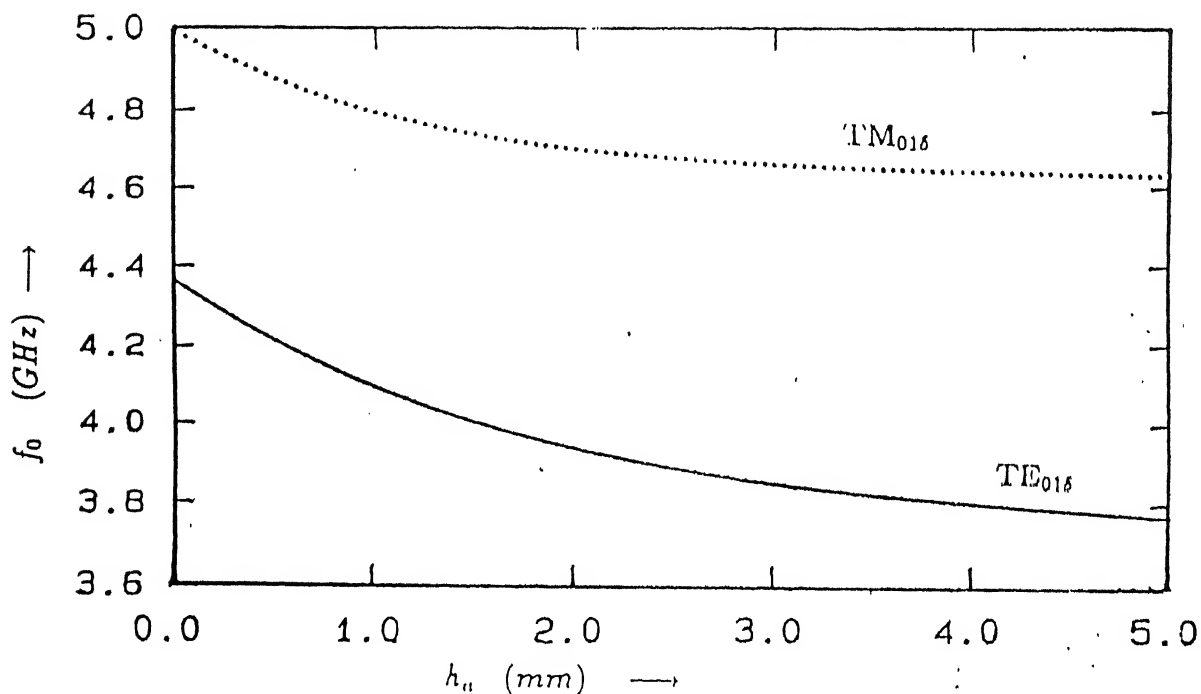


Figure 3.6: Mode chart for Cylindrical DR.

3.2 Theory of a Band Pass Filter.

Accurate Band Pass filter (BPF) design is important for realization of a mixer. Using the design data required to relate, external quality factor and coupling coefficient, physical specifications of the filter can be computed, in accordance with desired filter response.

Low pass prototype design and then transformation to desired frequency to realize required band pass response is a reliable and popular method [7]. For design, first it is necessary to choose an appropriate power loss function (like Butterworth or Tchebycheb functions etc.) in the pass band of the low pass prototype filter. Specification of this insertion loss or return loss for a lossless network (filter) is the next requirement. Once this is specified as the function of frequency the prototype values are chosen from the formulae given by Matthaei [7]. Now the low pass prototype values can be transformed into desired bandpass characteristics by using low pass to band pass transformations.

Matthaei also gives an equivalent circuit of a direct coupled band pass filter using

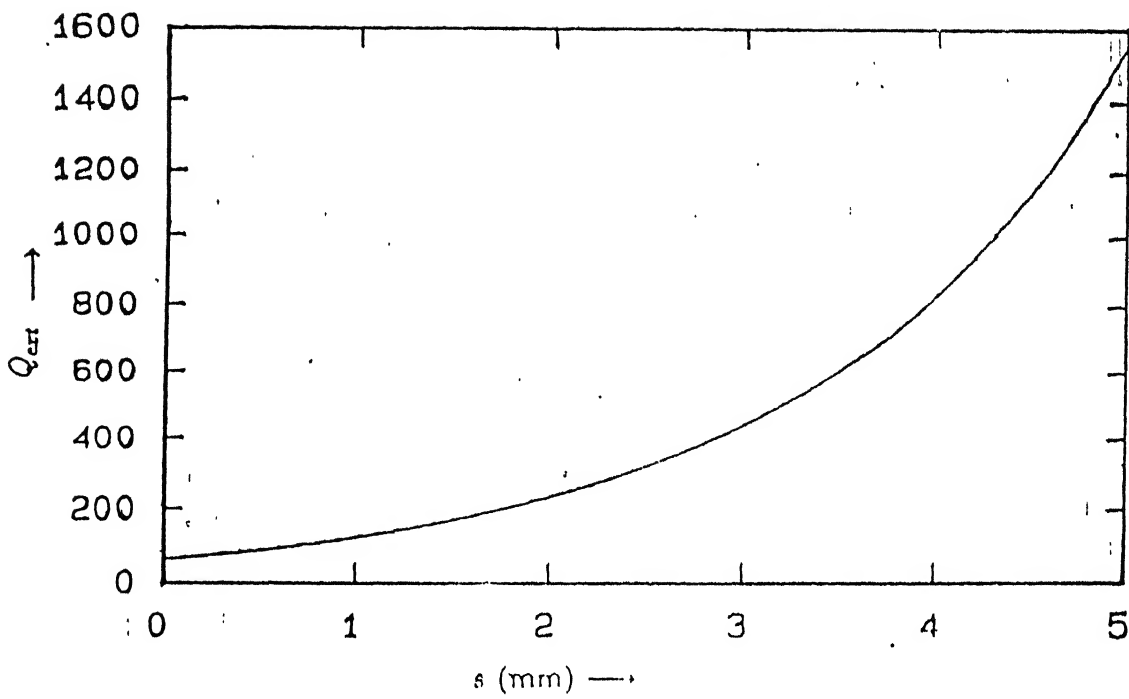


Figure 3.7: External Quality Factor.

impedance invertors as shown in fig. 3.10.

Input/output coupling for this circuit is represented by external quality factor $Q_{ext(a)}$ and $Q_{ext(b)}$ while coupling between resonators is represented by coupling coefficients $k_{j,j+1}$. These quantities can be found experimentally or can be computed in terms of low pass prototype g_i 's as given in the formulae below:

$$Q_{ext(a)} = \frac{X_1}{\frac{k_{0,1}^2}{R_a}} = \frac{g_0 g_1}{w} \quad (3.2)$$

$$Q_{ext(b)} = \frac{X_n}{\frac{k_{n,n+1}^2}{R_b}} = \frac{g_n g_{n+1}}{w} \quad (3.3)$$

$$k_{j,j+1} = \frac{K_{j,j+1}}{\sqrt{(X_j X_{j+1})}} = \frac{w}{\sqrt{(g_j g_{j+1})}} \quad j = 1, 2, 3 \dots, n-1. \quad (3.4)$$

here w is the fractional bandwidth given by $w = \frac{\omega_2 - \omega_1}{\omega_0}$ and $\omega_0 = \sqrt{(\omega_2 - \omega_1)}$.

The passband edges ω_2 and ω_1 are for Tchebycheb response defined by pass band ripple level. This information about Q_{ext} and k are useful in deriving the physical specifications i. e. microstrip line to DR (input-output coupling) and DR to DR coupling (interstage coupling) necessary for actual design.

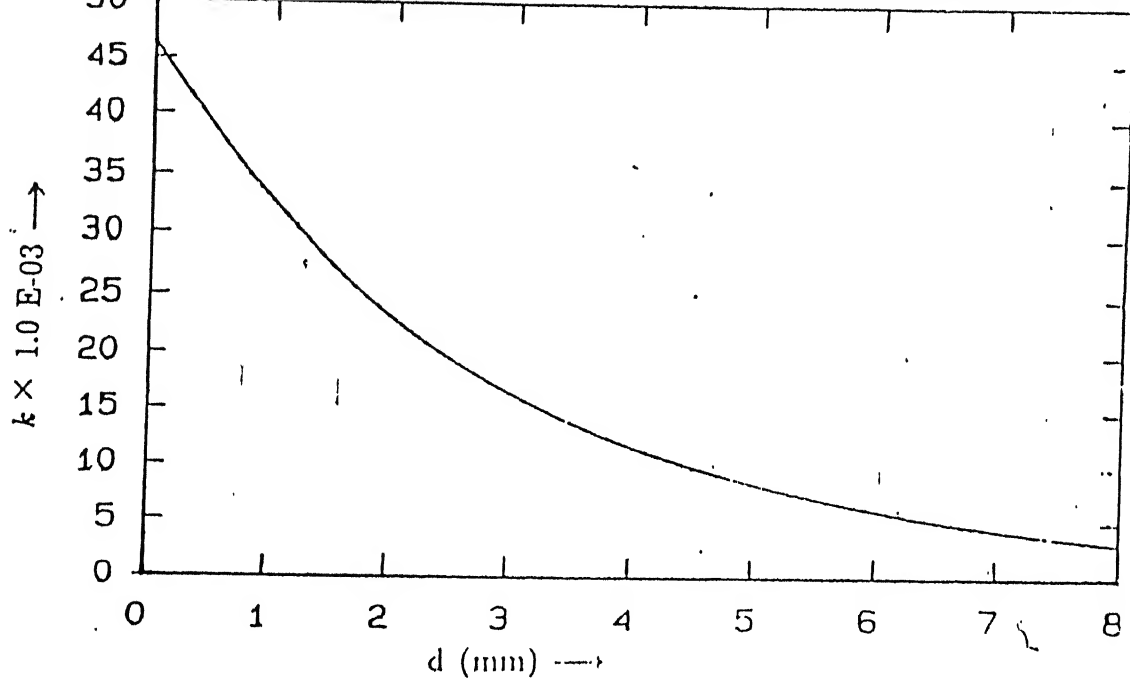


Figure 3.8: Coupling Coefficients.

3.3 Theory of Mixers

Mixers make use of non-linear characteristics of certain solid state devices to generate an output signal containing many frequency components. A simple analysis [11] shows how new frequencies are generated in non-linear circuits. Mixers basically convert the input frequency to a new frequency. Mixing is achieved by applying both the input r. f. (RF) signal and a local oscillator (LO) to a nonlinear device. LO is a higher power signal used to pump the nonlinear device. Taking the example of a diode, its I/V characteristics can be expanded via a power series and by assuming a multitone excitation generation of various frequency components can be amply demonstrated, as shown in succeeding paragraphs. For a diode dc voltage-current relationship is given as

$$i = I_s [\exp^{\alpha V_j} - 1] \quad (3.5)$$

where i = instantaneous current, I_s = diode saturation current,

V_j = instantaneous voltage across the junction,

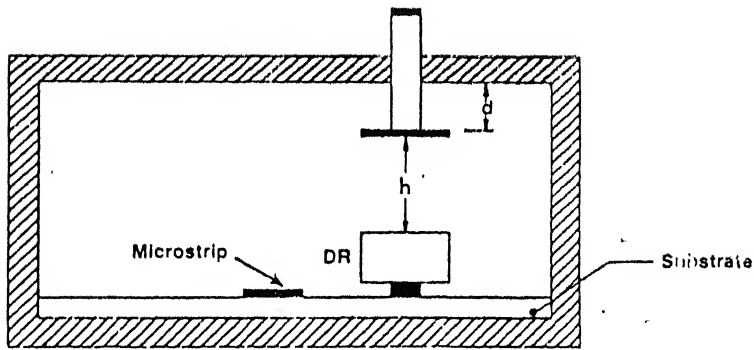


Figure 3.9: Mechanical Tuning.

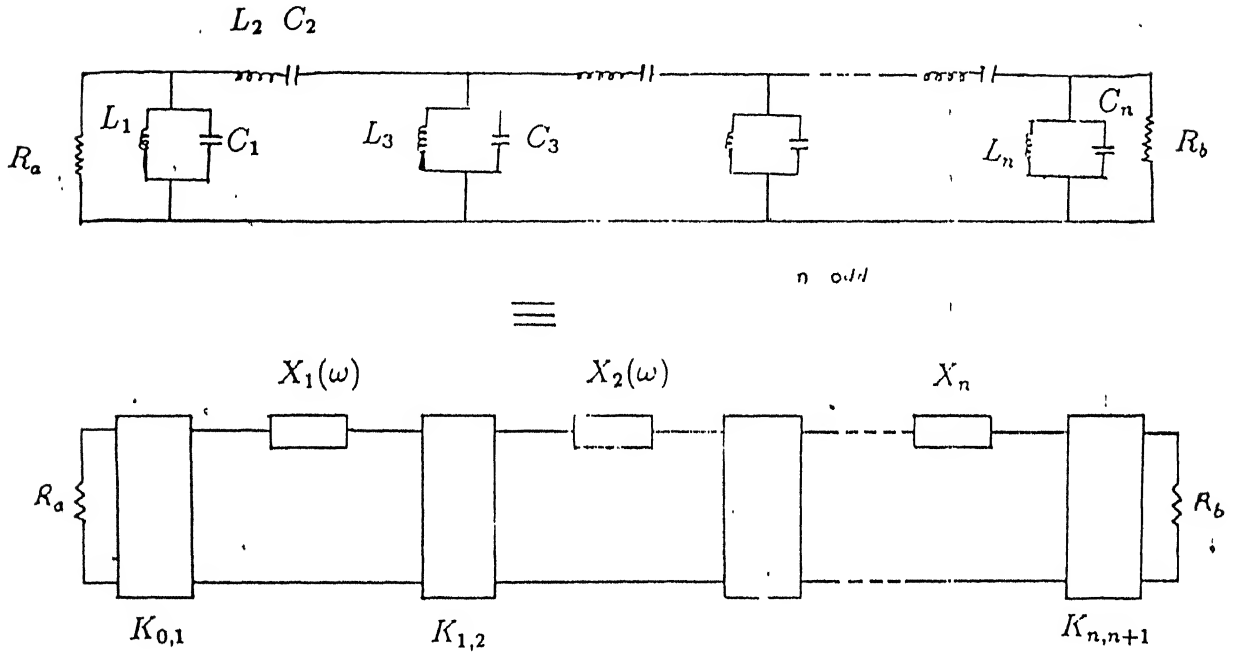


Figure 3.10: Equivalent circuit of a Band Pass Filter.

$\alpha = e/nkt$, where

e = electron charge

k = boltzmann constant

T = absolute temp

n = ideality factor typically 1 to 1.5.

For the case of a small applied ac voltage 3.5 can be expressed by the following power series

$$i = i(V_0 + \partial V) \quad (3.6)$$

where V_0 is the dc bias voltage,

I_0 is the dc or average bias current,

∂V is the ac voltage across diode junction.

$$i = i(V_0) + \partial V \frac{di}{dv} \big|_{I_0} + \frac{1}{2!} \partial V^2 \frac{d^2 i}{dv^2} \big|_{I_0} + \cdots + \frac{1}{n!} \partial V^n \frac{d^n i}{dv^n} \big|_{I_0} + \cdots \quad (3.7)$$

for

$$\partial V = V_1 \cos(\omega_1 t) + V_2 \cos(\omega_2 t) \quad (3.8)$$

where ω_1 is LO frequency, ω_2 is RF frequency, V_1 and V_2 are peak amplitudes of ω_1 and ω_2 respectively.

Substituting 3.8 in the power series expansion for instantaneous current and subtracting dc or average bias current eqn 3.7 and retaining uptill third order terms only, we get

$$i = i_a(t) + i_b(t) + i_c(t)$$

These have been obtained on applying the trigonometric formulae for squares and products of cosines. The first order terms are:

$$i_a(t) = a(V_1 \cos(\omega_1 t) + V_2 \cos(\omega_2 t)), \quad (3.9)$$

Second order terms are

$$\begin{aligned} i_b(t) = & b \left[\frac{1}{2} [V_1^2 + V_2^2 + V_1^2 \cos(2\omega_1 t) + V_2^2 \cos(2\omega_2 t)] \right. \\ & \left. + 2V_1 V_2 [\cos(\omega_1 + \omega_2)t + \cos(\omega_1 - \omega_2)t] \right] \end{aligned} \quad (3.10)$$

and the third order terms are as under

$$\begin{aligned} i_c(t) = & c [V_1^3 \cos(3\omega_1 t) + V_2^3 \cos(3\omega_2 t) \\ & + 3V_1^2 V_2 [\cos((2\omega_1 + \omega_2)t) + \cos((2\omega_1 - \omega_2)t)] \\ & + 3V_1 V_2^2 [\cos((\omega_1 + 2\omega_2)t) + \cos((\omega_1 - 2\omega_2)t)] \\ & + 6V_1 V_2 [\cos(\omega_1 + \omega_2)t + \cos(\omega_1 - \omega_2)t] \end{aligned}$$

$$\begin{aligned}
& +3V_1V_2^2[\cos((2\omega_2 + \omega_1)t) + \cos((2\omega_2 - \omega_1)t)] \\
& +3(V_1^3 + 2V_1V_2^2)\cos(\omega_1)t + 3(V_2^3 + 2V_2V_1^2)\cos(\omega_2)t] \quad (3.11)
\end{aligned}$$

In above current components a, b, c denote the incremental conductances about the dc operating point. As can be seen the total current, in the non-linear element is the sum of the current components in the three equations above. It consists of a large number of frequency components, each successive term in 3.7 is generating more such components. A closer examination shows that the generated frequencies are a linear combination of the two excitation frequencies.

$$\omega_{m,n} = m\omega_1 + n\omega_2 \quad (3.12)$$

where $m, n = \dots, -3, -2, -1, 0, 1, 2, 3, \dots$.

$\omega_{m,n}$ is called a *mixing frequency*, and the current component at that frequency is called a *mixing product*. The sum of the absolute values of m and n is called *order* of the mixing product. The m^{th} order mixing frequency is called m^{th} *harmonic* of the excitation frequency. The mixing frequency that arises as a linear combination of two or more tones is called *intermodulation product*.

Out of various components, the following are of greater importance:

IF ($\omega_0 = \omega_1 - \omega_2$), LO harmonics ($n\omega_1$), the image frequency ($2\omega_1 - \omega_2$), sum frequency ($\omega_s = \omega_1 + \omega_2$), and harmonic side bands $\omega_{sb} = n\omega_2 \pm \omega_1$.

Spurious responses in the form of unwanted harmonics and intermodulation products affect the performance of the mixer. As also resistive termination at the image, sum or harmonic sidebands results in loss of signal power that increases the mixer conversion loss. *Mixer conversion loss* l is defined as

$$l = 10 \log \left[\frac{P_{out}}{P_{av}} \right],$$

where P_{out} is power output at IF and P_{av} is power available at signal frequency.

3.3.1 Non linear solid state devices

In [11] modelling of non linear solid state devices has been dwelled upon in great detail. Such devices can be usefully represented using a lumped circuit model that includes both linear and non-linear resistors, capacitors and controlled sources.

A large number of non-linear solid state devices like *FET*, *GaAs MESFETs*, *schottky barrier junction diodes*, *schottky barrier varactors*, *p⁺n junction varactor*, and *step recovery diodes* can be used as mixers. Of these, use of schottky barrier junction diode and MESFETs as mixers has been dealt with, in succeeding paragraphs.

3.3.2 Schottky barrier diode

A schottky barrier diode consists of a metal contact deposited on a semiconductor. As shown in fig. 3.11 the diode is fabricated on a high conductivity n type (n^+) substrate; a very pure (n^+) buffer layer is grown on top of substrate.

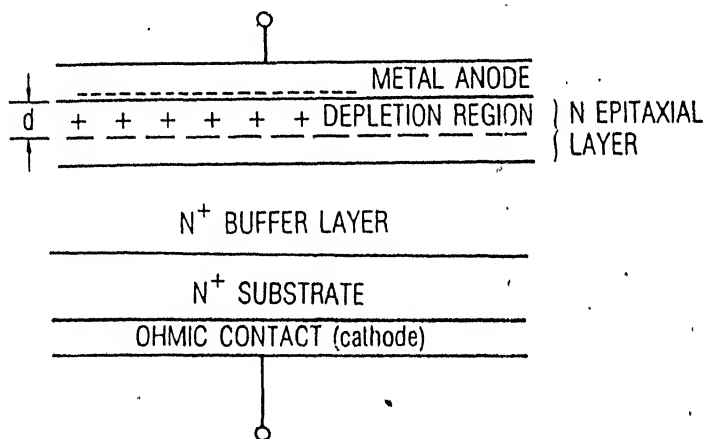


Figure 3.11: Schematic showing Schottky barrier Diode.

An n epitaxial layer is grown on top of buffer. The contact of metal anode to the epitaxial layer forms the rectifying junction.

The metal-semiconductor contact allows some free electrons in the semiconductor

to collect on the surface of the metal. A region of epitaxial layer, depleted of electrons, contains only positively charged donor ions. Presence of these ions, results in an electric field, which opposes the further movement of electrons. This field, now, results in a potential between the neutral semiconductor and the anode.

A reverse bias or a more negative voltage, across the diode, stores more negative charge on the anode and a forward bias reduces it. The junction, therefore, operates as a non-linear capacitor. As the forward bias increases, the electric field becomes weaker and presents a lesser barrier to electrons. The current is proportional to the number of electrons having greater energy than the barrier height.

A schottky barrier diode's equivalent circuit is shown in fig. 3.12 The diode is modelled to consist of three non-linear elements, the junction capacitance and conductance and the parasitic series resistance.

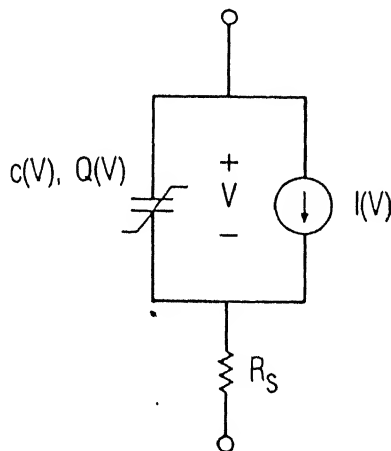


Figure 3.12: Equivalent Circuit of a Schottky Barrier Diode.

As it lacks minority carrier effects this is a very fast switching device and is ideal for use as a diode mixer. Very high quality silicon diodes are available at very low cost. *GaAs* schottky diodes can be obtained at a modest expense. Diode technology today, however, is sufficiently mature to allow mixers at frequencies above 1000 GHz [11].

3.3.3 GaAs MESFET

GaAs MESFET have revolutionized low-noise microwave electronics. They make excellent mixers, have low noise figure, broad bandwidth and conversion gain. Fig. 3.13 shows a cross section of a *GaAs MESFET*. It is fabricated by first growing a very pure, semi-insulating *GaAs* substrate, then growing an n-doped epitaxial layer that is used to realize the FET's active channel. Three connections are made to the FET these are: the source, the drain and the schottky barrier gate.

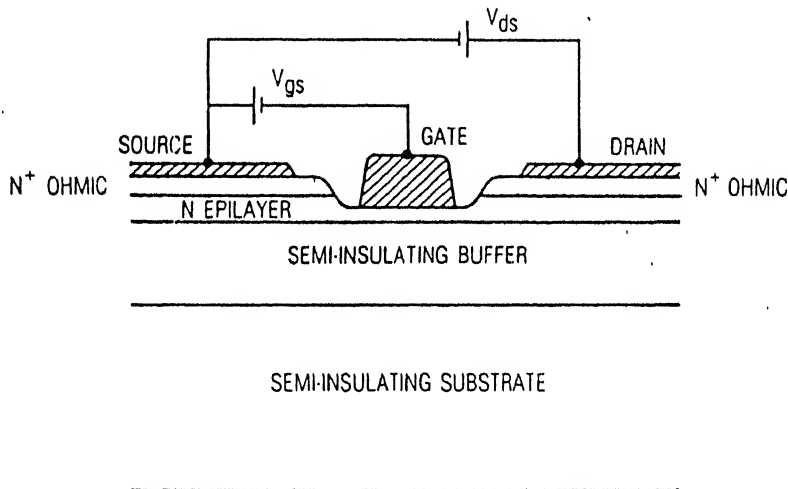


Figure 3.13: GaAs MESFET Schematic.

Two sources V_{gs} (gate-source) and V_{ds} (drain-source) bias the MESFET. These voltages control the channel current by varying the width of the gate depletion region and the longitudinal electric field. When V_{gs} is low, the current is approximately proportional to V_{ds} . If V_{gs} is increased while V_{ds} is constant the depletion region widens and conductive channel becomes narrower reducing the channel. Accurate non-linear FET analysis, involves controlled drain current source and gate channel capacitances. Gate channel capacitances are, in general non-linear and are functions of gate voltage and drain voltage. Many MESFET models have been proposed [11]. They differ primarily in the way in which they treat the charge domain and the controlled current

source modelling.

3.4 Types of Mixers

There are many types of mixers. These use one diode (single ended), two diodes (single balanced), four diodes (double balanced) or eight diode (double-double balanced). The mixer design issues can be addressed on the basis of a single diode and extended to other mixer configurations. Representative schematic diagrams are shown in fig. 3.14.

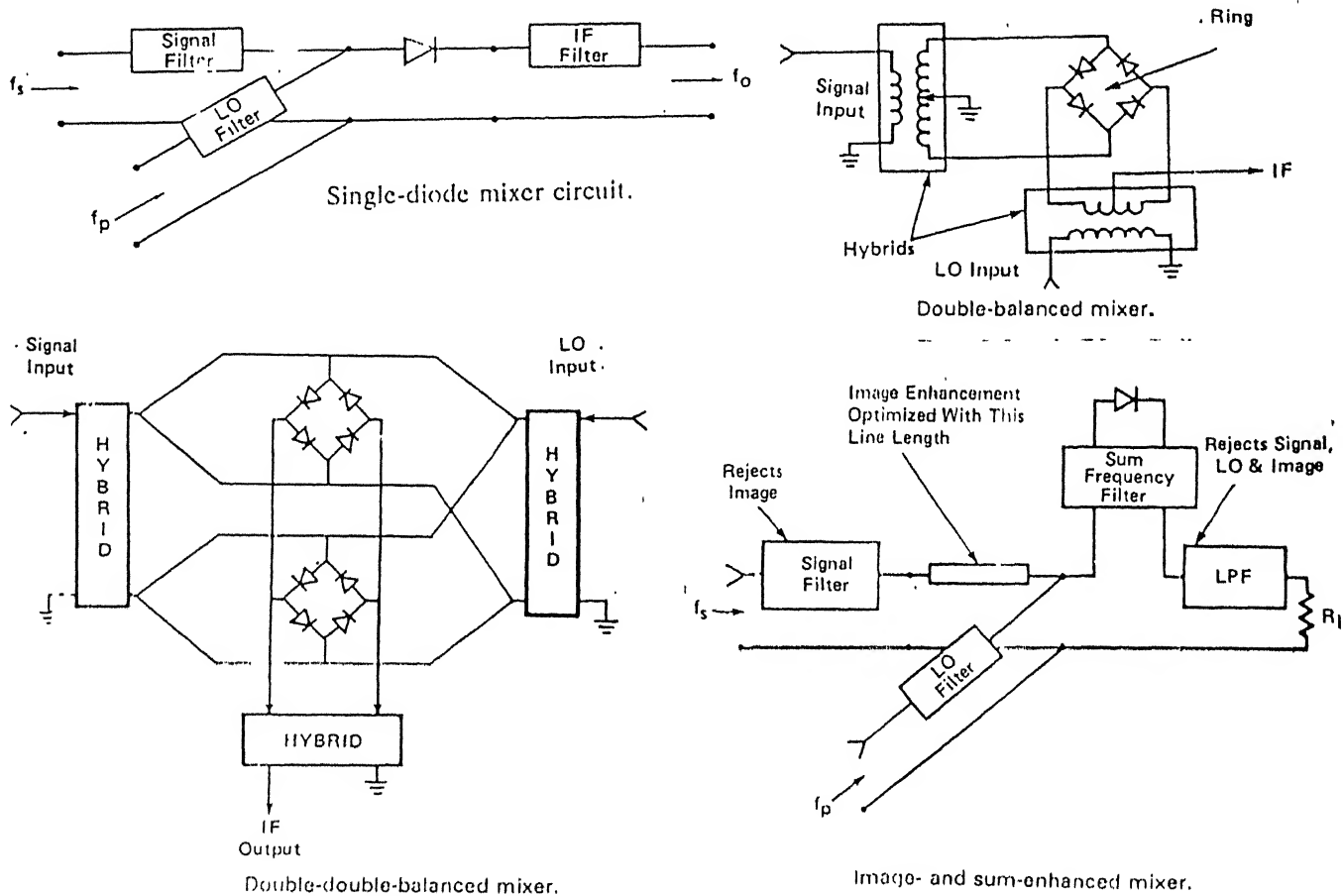


Figure 3.14: Various Types of Mixers.

There are also image rejection mixers and sum frequency enhanced mixers. The RF

band pass filter provides reactive terminations at the image frequency ($\omega_{im} = 2\omega_1 - \omega_2$) that must be properly phased so that reflected power at the image enhances the mixing process.

A single gate FET mixer can be realized as shown in fig. 3.15. The LO and RF are applied to the gate using a diplexer or a coupler; the IF is taken from the drain. The LO voltage serves to pump the FET and input matching circuit transforms the hyperbolic mean of the FET's two impedance states to 50 ohms.

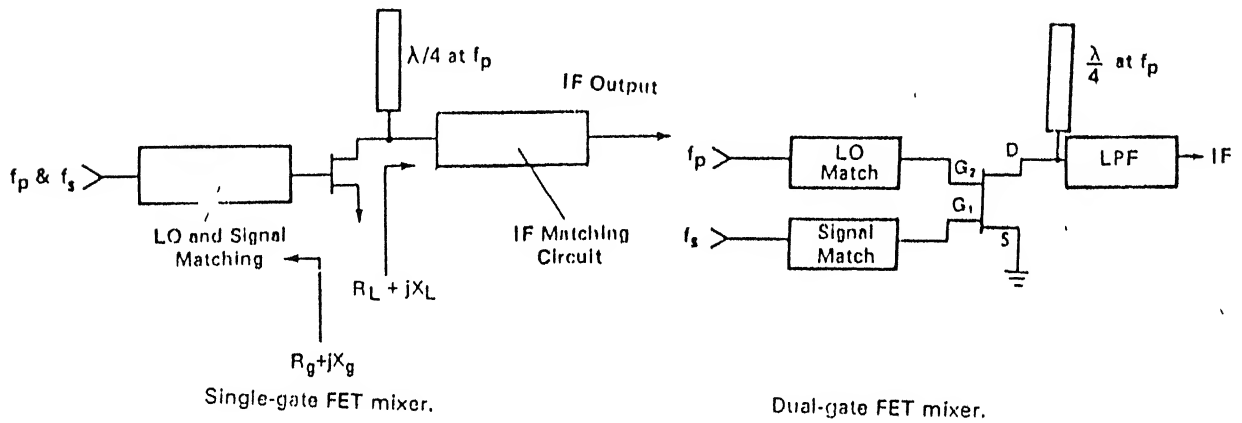


Figure 3.15: FET Mixer.

The conversion gain provided by the FET mixers, is the principal advantage over diode mixers. This gain reduces the overall noise figure of the circuit, however due to upconversion of low frequency noise resulting from gate capacitance modulation, noise figure of a FET mixer is higher than the case where it is used as an amplifier.

Single gate mixers can be realized by applying LO to the FET drain [4]. Dual gate FET mixers can provide higher conversion gain than single gate FET.

Also of extreme importance is proper design of input and output impedance matching circuits. [4,13] discuss a few of such techniques.

3.5 DR based Image recovery mixer

Imai and Nakakita in [1] propose an image recovery mixer wherein the signal and local oscillator BPF's use the DRs. A GaAs schottky barrier mixer diode has been used by the authors, at the end of the microstrip line. The microstrip line is magnetically coupled to DR's excited in cylindrical $TE_{01\delta}$ mode. For tight coupling between the microstrip lines and DRs, the DR's are placed at odd number multiples of a quarter of a guided wavelength at their resonant frequency from the open end of the microstrips.

Fig. 3.16 shows the schematic of the layout suggested by Imai.

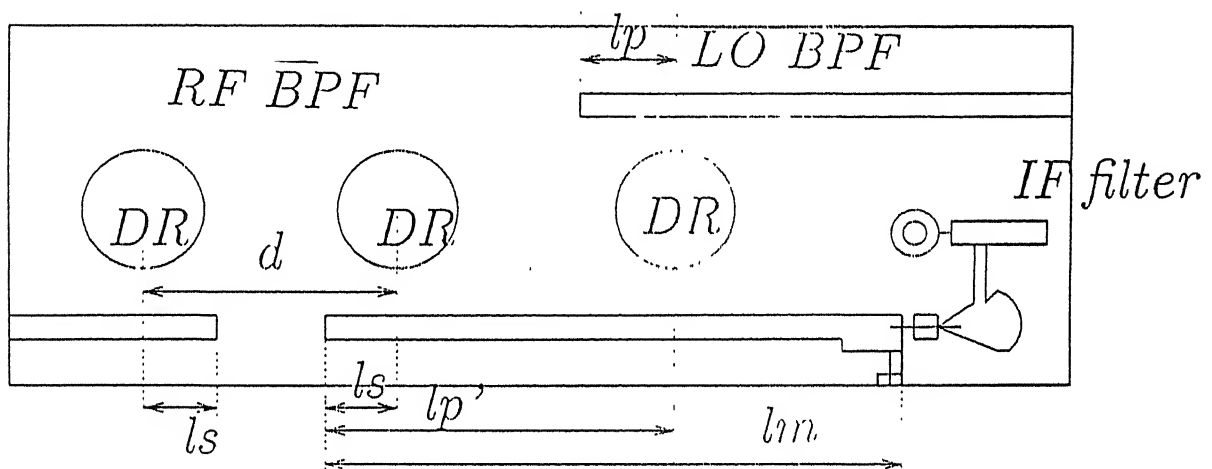


Figure 3.16: Schematic of proposed Layout.

In this layout, $l_s = \frac{\lambda_{gs}}{4}$, $l_p = \frac{\lambda_{gp}}{4}$, and $l_{p'} = \frac{7\lambda_{gp}}{4}$ where λ_{gs} and λ_{gp} are the guided wavelength of the microstrip line at the signal frequency and that of the local frequency respectively. In order to lower the noise figure, the impedance of the external circuits of the mixer diode should be nearly zero at the image frequency. This condition is achieved by keeping length l_m of microstrip line connected to the mixer diode as an odd number multiple of $\frac{\lambda_{gm}}{4}$, where λ_{gm} is the guided wavelength of the microstripline at the image frequency.

DRs for the RF BPF and LO BPF are magnetically coupled to this line, but the

impedance of the line seen from the diode at the image frequency is decided solely by the length l_m when Q_0 of DRs are sufficiently high they are completely off tuned at the image frequency. Thus the construction of DR's in this mixer does not destroy the image short condition.

Thus it can be seen that, implementation of a DR based mixer at the desired frequency requires the following:

- microstrip line design parameters,
- DR of desired resonant frequency,
- input/output and interstage coupling information.

Having seen all the necessary aspects of DR based mixer, the realization of a mixer has been given in the next chapter.

Chapter 4

DR BASED MIXER REALIZATION

This chapter deals with the realization of a mixer using DR's in MIC environment. DR's primarily find a place in realization of RF BPF and LO BPF.

Synthesis of a DR based mixer is quite involved. It is seen that the overall design problem can be suitably broken down as under:

- outline design decisions,
- calculation of transmission line parameters,
- input-output and interstage coupling information,
- design of band pass filter for RF and LO signal,
- impedance matching circuit for nonlinear device,
- layout and fabrication,
- tuning and performance improvement.

4.1 Outline design decisions

Various factors which would influence the outline design are:

- mixer specifications,
- filter specifications,
- input/output and interstage coupling information,
- transmission line design information,
- housing,
- components.

Using the transmission line design information and available coupling information, a mixer was to be realized with RF as 3.96 GHz. and LO frequency as 3.80 GHz. The filters were to be based on DRs. Three DRs were available, however necessary connectors and mixer diode were collected from IIT Delhi.

In the present realization, of the three available DRs, two were used for RF band pass filter and one for LO band pass filter realization. A copper housing has been fabricated to house the circuitry. The components have been laid out on a RT/duroid substrate. SMA connectors have been used to launch power into the circuits. A silicon schottky barrier mixer diode is used, as the non-linear mixing device.

4.2 Transmission line parameters

Using the expressions developed in *chapter two* various parameters required for accurate design of microstrip line were generated. These have been tabulated in table 4.1 The characteristics of the substrate used were $\epsilon_r = 2.18$ and thickness of the substrate was $d = 0.8mm$.

$w(mm)$	$Z_0\Omega$	$f_0 GHz$	$\lambda_0 (mm)$	$\frac{\lambda_g}{\lambda_0}$	λ_g
2.4	50.659	3.96	75.706	0.72957	55.232
2.4	50.654	3.80	78.892	0.7396	57.565
2.4	50.650	3.64	82.36	0.7297	60.101
0.5	112.28	3.96	75.705	0.7527	56.983

Table 4.1: Transmission line Data.

4.3 Band pass filter design

4.3.1 RF BPF design

Having fixed the number of DR's to be used as 2, filter specifications chosen are as under

Response: Tchebycheb with 0.5 dB ripple in pass band.

Centre frequency: 3.96 GHz.

3dB BW: 70 MHz.

Stop band attenuation greater than 20 dB.

Disc type resonators, chosen for the design have following electrical and physical parameters:

Height $h = 6.66$ mm

Diameter $2a = 15.07$ mm

Dielectric constant $\epsilon_r = 37.8$

Unloaded Quality factor $Q_u = 6000$

Value of aspect ratio $= 2.252$.

Following the method given by mathaci [7] for the specifications given above various design data obtained are

number of resonators = 2

$$g_0 = 1$$

$$g_1 = 1.4029$$

$$g_2 = 0.7071$$

$$g_3 = 1.9841$$

$$\omega_1 = 3.925GHz, \text{ and } \omega_2 = 3.995GHz.$$

using equation 3.2 to 3.4 we obtain

$$Q_{ext}(a) = \frac{g_0 g_1}{w} = 79.360$$

$$Q_{ext}(b) = \frac{g_2 g_3}{w} = 79.364$$

$$w = 0.0176$$

$$K_{1,2} = 0.017748$$

From the design curves given in fig. 3.7 and fig. 3.8 distance between the DR and microstrip line works out to 2.812 mm. and the distance between two DRs works out to 0.4 mm.

4.3.2 LO BPF Design

The number of resonators to be used is one. Centre frequency is $3.80GHz$. Low pass filter parameter are as under:

$$g_0 = 1.0$$

$$g_1 = 0.6986$$

$$g_2 = 1.0$$

$$\omega_1 = 3.79GHz,$$

and $\omega_2 = 3.81GHz$. using equation 3.2 to 3.4 we obtain

$$Q_{ext}(a) = Q_{ext}b = 132.7335.$$

From design curves in fig. 3.7, the design distance between the DR and the micro-

strip line works out to 1.12 mm.

4.3.3 Impedence matching for the Diode

HP schottky barrier mixer diode no 5082 – 2580 is used as the non-linear device. The diode is used in self bias mode. A very thin line is used to complete the DC path.

Smith chart was used to calculate the stublength of a open circuit stub for matching the input impedance of the diode to a 50Ω line. From the manufactures data sheet the impedance of the diode was $\bar{y} = 1.2 - j0.85$

Impedence to be matched worked out to

$Z = 28 + j19.7\Omega$. This was matched using a open circuit stub of length 0.108λ placed at 0.1725λ from the diode's point of contact.

4.4 Mixer design

Based on the physical dimensions obtained above a copper housing was prepared to house the above circuits. The dimensions of the housing chosen were to be such that it did not act as a waveguide at the required frequency. From table 4.1 the microstrip line lengths required for design were evaluated as under

$$l_s = 13.808mm$$

$$l_p = 14.391mm$$

$$l_{p'} = 71.955mm$$

$$l_m = 105.178mm$$

This ensured that DRs were placed near the point of maximum current and image short condition is achieved. A suitable layout was arrived at and the microstrip line line was printed. Fig. 4.1 shows the layout of the designed mixer.

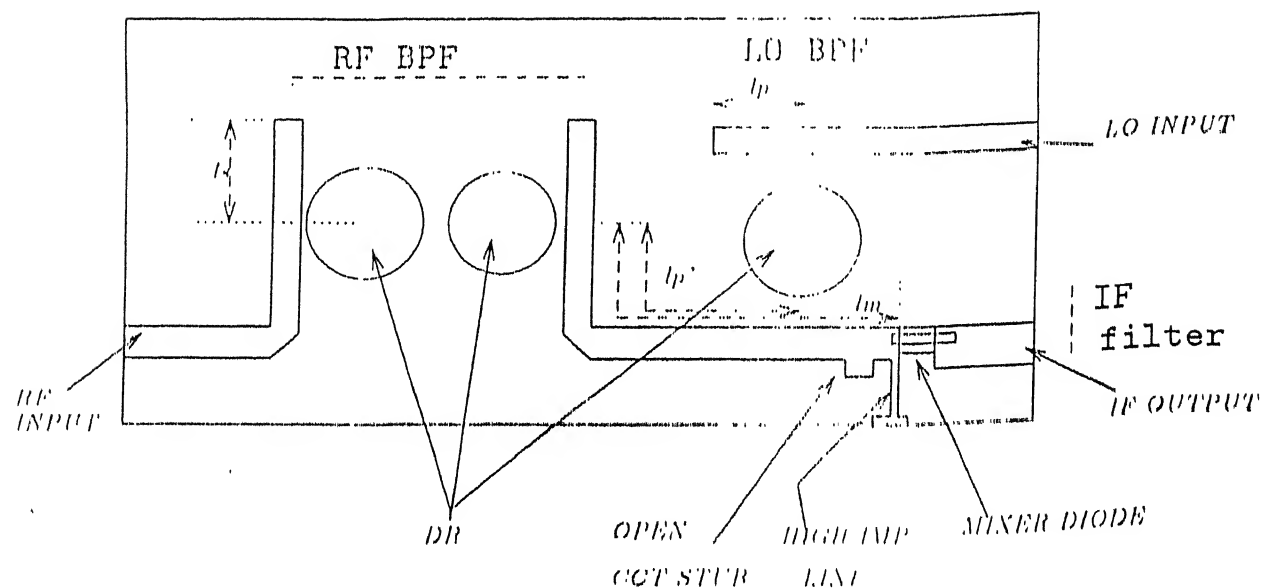


Figure 4.1: Layout of the Designed Mixer.

For IF filter design a broad patch has been used at the output of the diode. A thin high impedance line is used for providing dc path for the diode to work in self bias mode.

4.5 Tuning and performance improvement

To improve the performance of the mixer two tunable screws were placed directly at the top of the DRs to tune the resonant frequency. Better spurious response suppression was achieved by physically placing another open circuit stub physically at a suitable place. Exact size aluminium spacers were made to raise the height of the top plate for better tunability.

The mixer Noise Figure and conversion loss are as shown in fig. 4.2 and 4.3 respectively. $|S_{11}|$ at RF port is shown in fig. 4.4. The mixer output was found to be narrow band and virtually all the spurious harmonics are suppressed. Initially noise figure achieved was very poor. Improvement in noise figure was achieved by repositioning the

<i>Parameter</i>	<i>Measured Value</i>
LO-IF Isolation	$> 32dB$
RF-IF Isolation	$> 42dB$
Noise Figure	$12dB$
3 dB IF Bandwidth	$40MHz$
20 dB RF BPF BW	$140MHz$
Conversion Loss	$15\ dB$

Table 4.2: Performance Data.

DRs on the substrate. Some improvement in coupling was achieved by placing small capacitances around the DRs.

The $|S_{11}|$ and $|S_{21}|$ were found to be very susceptible to positioning of DR and height of top plate. By varying the height of the top plate entire band of frequencies could be shifted to left or right on the frequency axis.

Misc. performance data is given in table 4.2.

A photograph showing the layout of designed structure is shown at fig. 4.5.

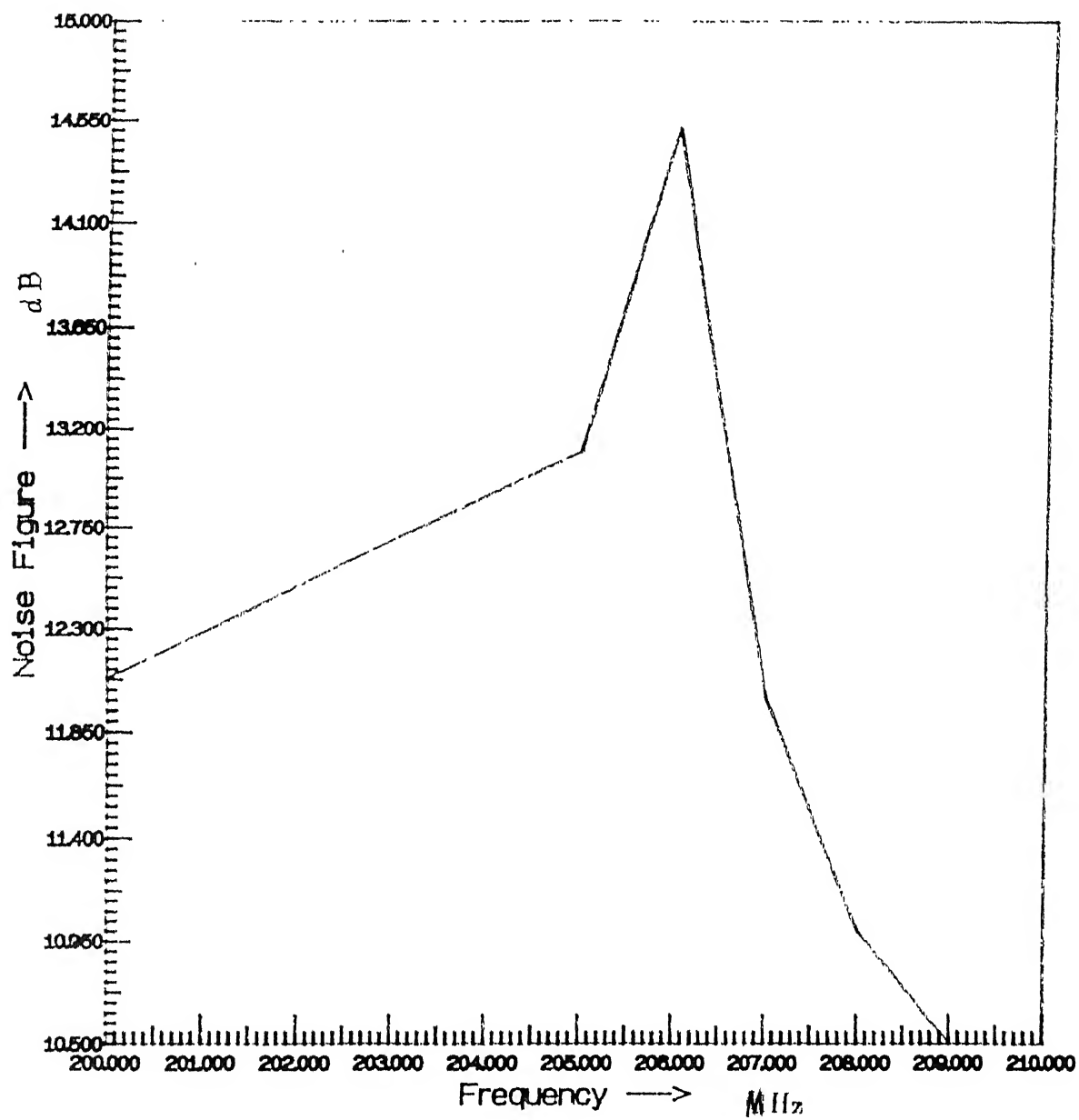


Figure 4.2: Noise Figure.

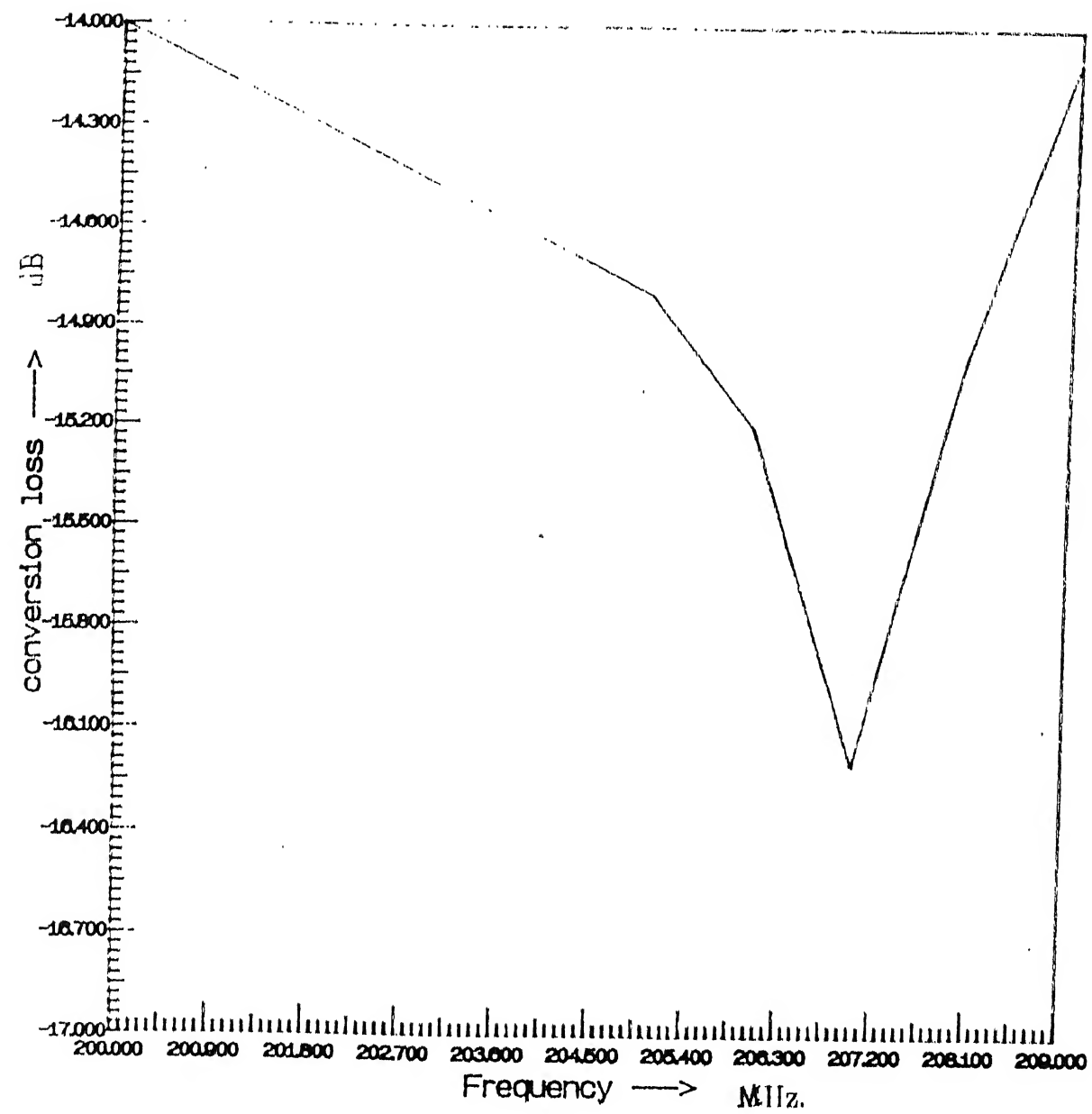


Figure 4.3: Conversion Loss.

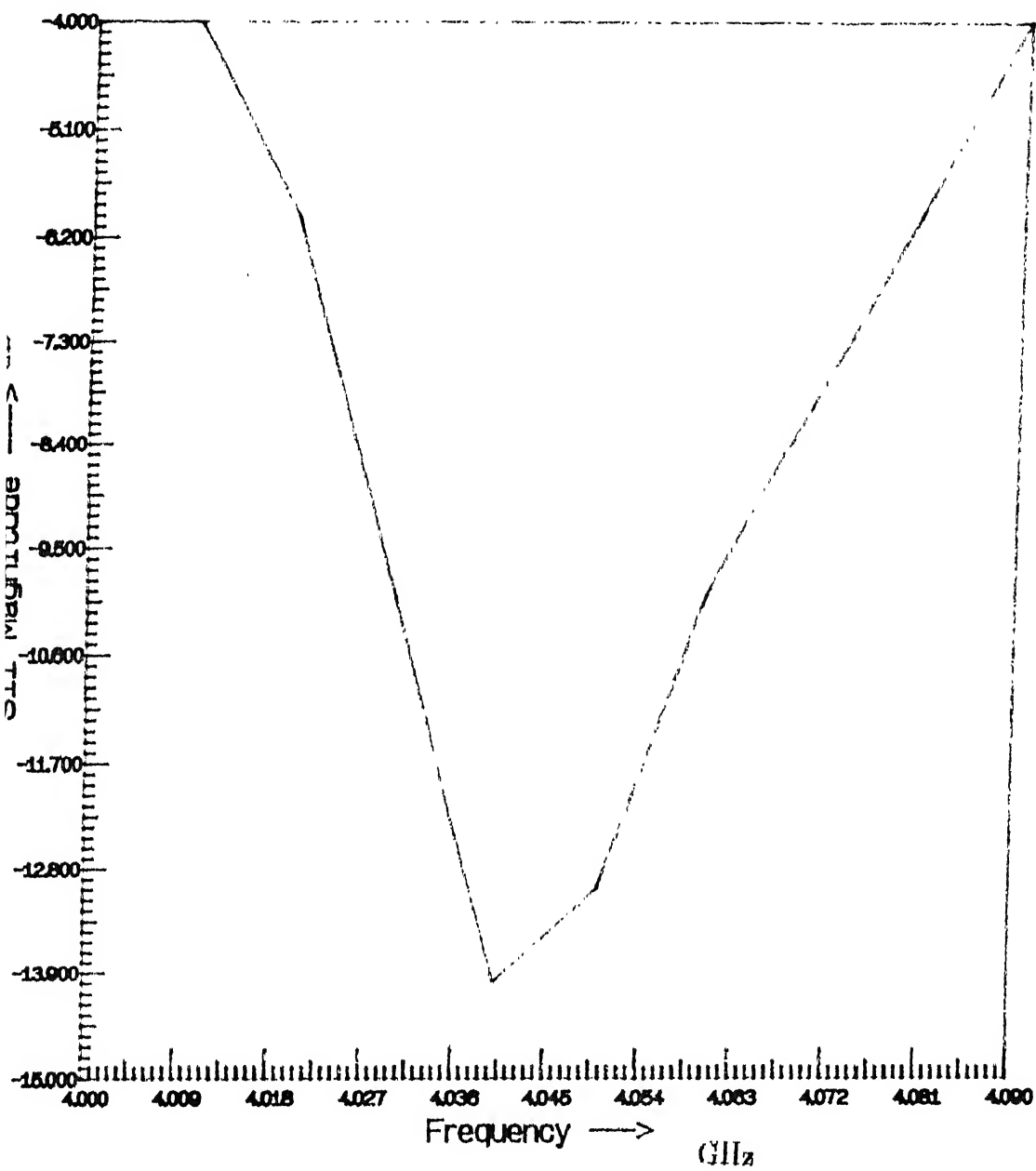


Figure 4.4: $|S_{11}|$ at RF Port.

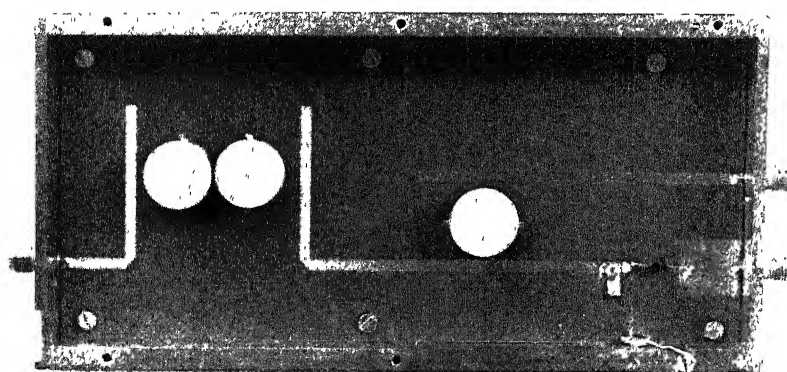


Figure 4.5: Photograph showing the top view of the C Band Mixer.

Chapter 5

CONCLUSION AND FUTURE DEVELOPMENTS

Accurate formulation of transmission line design in MIC environment was quite important, as these results coupled with the coupling information from [8] present a formidable design tool towards an accurate and reliable DR based filter design. Iterative fabrication and testing would further vindicate such an approach, however it would require a free availability of components.

Importance of individually prototyping and testing each of the subcomponents also emerged. Such an approach would lead to a cut down in overall design time.

An effort was made in this thesis to arrive at and validate a methodology for design of cylindrical DR based mixer in MIC environment. The results achieved show that it is a feasible design approach. Improved performance can certainly be obtained using GaAs MESFETs as the non-linear devices.

References

- [1] K. Imai and H. Nakakita. A 22 GHz Band Low noise down convertor for satellite receivers *IEEE Trans. Microwave Theory Tech.*, Vol. 39, pp.993-999, June 1991.
- [2] Y. Utsuni and K. Imai. 22 GHz band low noise down down convertor for sattellite broadcasting *IEEE Trans. Broadcast.*, Vol. BC-30, pp.1-7, Mar. 1984.
- [3] B. Bhat and S. K. Koul. *Analysis, Design and Application of Fin Lines* Artech House INC., Norwood MA 02062, 1988.
- [4] I. Bahl and P. Bhartiã. *Microwave Solid State Circuit Design*. John Wiley & Sons Inc., Canada, 1988.
- [5] D. J. Masse, et al. A New low-loss High-K temperture compensated Dielectric for Microwave applications. *Proc. IEEE*, Vol. 59, pp.1628-1629, Nov. 1971.
- [6] D. Kajfej and P. Guillon. *Dielectric Resonator*. Artech House, Dedham, Mass., 1986.
- [7] G. L. Matthai, L. Young, and E. M. T. Jones. *Matching Networks and Coupling structures*. McGraw-Hill, New York, 1964.
- [8] A. Jain. Studies on dielectric resonator and design of a band pass filter in MIC environment. *M. Tech. Thesis* , IIT Kanpur, Nov. 1993.

- [9] Y. Komatsu and Y. Murakami. Coupling coefficient between microstrip line and dielectric resonator *IEEE Trans. Microwave Theory Tech.*, Vol. 31, pp.34–40, Jan. 1983.
- [10] P. Skalicky. Direct coupling between dielectric resonators *Electron. Lett.*, Vol. 18, pp.332-334, 15 April 1982.
- [11] S. A. Maas *Nonlinear Microwave Circuits* Artech House INC., Norwood MA02062, 1988.
- [12] Stegun, et. al. *Handbook of Mathematical Functions* Dover Publications, INC., New York, 1972.
- [13] P. C. L. Yip. *High Frequency Circuit Design and Measurements* Chapman and Hall, London, UK, 1990.

1286

EE-1995-M-ARO-DES